CALIFORNIA STATE UNIVERSITY SAN MARCOS

THESIS SIGNATURE PAGE

THESIS SUBMITTED IN PARTIAL FULFILLMENT
OF THE REQUIREMENTS FOR THE DEGREE

MASTER OF SCIENCE

IN

BIOLOGICAL SCIENCES

THESIS TITLE: The Impact of Obesity on Intestinal Epithelial T Cell Number and Function in Mice at Different Stages of Maturity

AUTHOR: Christa S. Park

DATE OF SUCCESSFUL DEFENSE: 08/07/17

THE THESIS HAS BEEN ACCEPTED BY THE THESIS COMMITTEE IN PARTIAL FULFILLMENT OF THE REQUIREMENTS FOR THE DEGREE OF MASTER OF SCIENCE IN BIOLOGICAL SCIENCES.

Julie Jameson THESIS COMMITTEE CHAIR	SIGNATURE	8/9/17 DATE
Deborah Kristan THESIS COMMITTEE MEMBER	SIGNATURE	8/7/17 DATE
Kimberly D'Anna Hernandez THESIS COMMITTEE MEMBER	SIGNATURE	8/7/17 DATE

The Impact of Obesity on Intestinal Epithelial T Cell Number and Function in Mice at Different Stages of Maturity

Christa S. Park

Department of Biological Science

California State University San Marcos

San Marcos, CA 92096

Thesis Committee:

Dr. Julie Jameson (Chair)

Dr. Deborah Kristan

Dr. Kimberly D'Anna-Hernandez

Table of Contents

Abstract

According to the Journal of the American Medical Association and the Centers for Disease Control and Prevention, one in six children and adolescents in the United States are obese. Obesity is a metabolic disease caused by a caloric imbalance, which leads to an accumulation of excess fat in the body. Adipose tissue constitutes an endocrine organ that can become unregulated as it expands and cause chronic systemic inflammation. There is a strong correlation between obesity and inflammatory conditions such as inflammatory bowel disease. In addition, the gastrointestinal problems encountered in obese youth are more severe than in patients whose obesity manifests in adulthood. Although intraepithelial lymphocytes are known to improve intestinal barrier function and decrease the severity of inflammatory bowel disease, it is unknown whether intraepithelial lymphocytes are impacted by obesity. An established murine model of obesity was used to examine the relationship between the developmental stage of obesity onset and the ability of intraepithelial lymphocytes to seed in the intestine, maintain normal numbers and function in barrier protection. Since intraepithelial lymphocytes seed in the intestine early in childhood and proliferate locally to produce numbers that are maintained throughout adulthood, we hypothesized that these immune cells may be especially sensitive to obesity at an early age. Immunohistochemistry and flow cytometry were used to examine intraepithelial T cell number and function in the intestine of mice that experienced controlled onsets of obesity at stages similar to child, adolescence, and adulthood of humans. Intraepithelial lymphocytes were significantly reduced in all three stages of maturation after consuming a high fat diet. Obese weanling mice exhibited the fewest intraepithelial lymphocytes as compared to the obese adolescent and obese adult mice. However, T cell subsets in adolescent and adult mice were more severely skewed toward inflammatory populations with elevated TNF-α production

than T cell subsets in weanling mice. Both factors may result in problems with barrier function and contribute to the increased severity of inflammatory bowel disease. Together these results demonstrate that the age at which weight gain is initiated is important in the pathogenesis of intestinal disease in obesity.

Obesity in the United States

Obesity has reached an epidemic level in the United States. Nearly one in three adults and one in six children and adolescents are obese (Ogden et al. 2014). Obesity in adults is defined as having a body mass index (BMI) of 30 kg/m^2 or greater (Flegal et al. 2002, Ogden et al. 2014, Pi-Sunyer et al. 2002) while obesity in children is defined as having a BMI at or above the 95% percentile of a specified reference population determined by the Centers for Disease Control and Prevention (CDC) growth charts (Ogden 2010). The number of obese American children between ages 6 to 11 has increased from 7% in 1980 to nearly 18% in 2010. Similarly, the percentage of obese adolescents between ages 12 to 19 has increased from 5% to 19% over the same time period. To put this into perspective, there are 12.5 million American children and adolescents who are clinically obese (Flegal et al. 2012, Ogden et al. 2014). Consequently, in 2008 alone, $147 billion was spent to treat health complications related to obesity (Finkelstein et al. 2009). In general, obese patients average $1,429 more in medical costs per year compared to patients with a healthy BMI (Finkelstein et al. 2009). Studies have shown childhood obesity increases the likelihood of adult obesity (Whitlock et al. 2005). This health crisis is a huge detriment to the US economy and the well-being of our future generations. Thus, the impact of obesity on human health can no longer be overlooked.

Obesity is the result of a habitual imbalance between food intake and energy expenditure (Speakman 2006, Hill et al. 2012). There are a variety of factors that shift this balance away from a healthy BMI. When more calories are consumed than can be metabolized, body mass increases. Generally in the US population, the primary source for excess calories is from overconsumption of foods with high fat and/or high carbohydrate content (Horton et al. 1995). Additionally, limited energy expenditure can increase the likelihood of obesity. Individuals who rarely

exercise are shown to be more prone to poor physical and mental health (Hennessy et al. 1994). On the other hand, there is a positive relationship between physical activity and health-related quality of life (Brown et al. 2014). Furthermore, patients may have a genetic predisposition to obesity that becomes exacerbated under certain environmental conditions (Millington 2013). In Western countries, exposure to high-fat diets and sedentary lifestyle is common. Subsequently, individuals living in such conditions are more prone to obesity, which in turn, escalates the number of health related illnesses each year due to accumulation of excess adipose fat tissue (Pi-Sunyer 2002, Residori et al. 2003, Speakman 2006). There are many clinical health risks and comorbidities associated with having a high body-mass index, including hypertension, dyslipidemia, diabetes mellitus, coronary heart disease, heart failure, stroke, gallstones, osteoarthritis, cancer, and decreased fertility (Residori et al. 2003, Pi-Sunyer 2002, Rees 2009).

Obesity also compromises barrier tissue function in the intestinal epithelium. Adults suffering from both obesity and inflammatory bowel disease (IBD) experience more severe inflammation than those who suffer from IBD alone. The adverse effects of these diseases combined, leads to increased anoperineal complications (Blain et al. 2002). Epidemiological studies indicate that of the children between the ages of 2 to 18 described in IBD cases, 24% are overweight or obese. Of the population of children who are affected by Crohn's disease, 20% are overweight or obese, and of the population of children affected by ulcerative colitis, 30% are overweight or obese (Long et al. 2011). The studies however, have yet to discern a causative relationship between obesity and IBD in children.

Individuals who maintain persistently high levels of excess adipose tissue and experience systemic chronic inflammation can experience epithelial barrier tissue dysfunction in the skin as well. Obesity increases susceptibility to chronic non-healing wounds and infection, which may

result in amputation or surgical debridement (Skrepnek et al. 2014, Pickwell et al. 2015). Systemic inflammation associated with obesity correlates closely with a loss of barrier tissue integrity and dysfunction of tight junctions between the epidermal cells of the skin, resulting in transepidermal water loss (Guida et al. 2010, Loffler et al. 2002). Our laboratory has also shown in obese mouse models and *in vitro* that obesity is detrimental to skin-resident T cell number and function. A loss of skin-resident T cell number and/or function leads to a substantial reduction in rates of wound healing in epidermal tissues (Jameson et al. 2002, Taylor et al. 2011). We have attributed at least some of the defects in T cell function to chronic inflammation that is associated with obesity (Taylor et al. 2011).

Chronic inflammation in obesity

As fat storage increases, a chain of events leads to altered T cell populations, which ultimately result in chronic systemic inflammation (Kern et al. 2001, Duffaut 2009). First, there is an accumulation of cytotoxic CD8+ T cells that attract macrophages to the excess adipocytes. These CD8+ T cells and macrophages are stimulated by cytokines produced by the adipocytes, and in turn begin to produce granzyme B, interferon gamma (IFN-γ), and chemokines of their own. The macrophages that surround the fat cells create a "crown like" structure, which produces inflammatory mediators such as tumor necrosis factor-alpha (TNF-α), interleukin-1 beta (IL-1β), and interleukin-6 (IL-6) to recruit additional CD8+ T cells (Weisberg et al 2003, Murano 2008, Clark et al. 2005, Kern et al. 2001, Halle et al. 2004). As a result, a combination of inflammatory promoters from adipocytes, CD8+ T cells, and macrophages all perpetuate one another, leading to systemic inflammation and insulin resistance in the chronically obese (Yang et al. 2010, Nishimura et al. 2009). Furthermore, obesity increases the expression of inflammatory genes

such as leptin and IκB kinaseβ (IKKβ) which are involved in obesity induced insulin resistance (Xu et al. 2003, Greenberg and Obin 2006).

Inflammation is further exacerbated by increased production of the proinflammatory cytokine, interleukin-17 (IL-17), by γδ T cells in the adipose tissue. IL-17 is important in glucose metabolism and adipogenesis (Zuniga et al. 2011). In addition to IL-17, IFN-γ plays a key role in the chronic inflammation associated with obesity. Obese IFN-γ deficient mice have reduced levels of inflammatory mediators such as TNF-α and monocyte chemoattractant protein-1 in their adipose tissue and have enhanced glucose tolerance that protects them from inflammation and insulin resistance (Rocha et al. 2008). Thus, T cells can also display pathological functions in an obese environment by producing IFN-γ, which disrupts the regulation of the inflammatory response.

Under obese conditions, CD8+ T cells, γδ T cells, and macrophages localized around adipocytes are highly stimulated. This stimulation however, is not limited locally to adipocytes, as other systemic immune cells are also affected. Thymic involution occurs at a younger age in obese mice, resulting in a less diverse T cell repertoire and a decreased overall T-cell count (Yang et al. 2010). Obese patients exhibit changes in peripheral T cell numbers and are shown to have an increased CD4+ T cell population and a decreased CD8+ T cell population, which can impede tumor surveillance (O'Rourke et al. 2005). Furthermore, Foxp3+ T regulatory cells (Tregs), which are important in controlling inflammation, are also reduced in the fat tissue of obese mice (Feuerer et al. 2009). It is speculated that this reduction in Tregs is due to a decrease in the amount of TGF-β produced by γδ T cells, which is essential for Treg proliferation (Taylor et al. 2010, Chen et al. 2003). A reduction of Tregs is detrimental to the intestine since Tregs play a key role in preventing inflammatory bowel disease. When HIF-α knockout mice were

administered dextran sulphate sodium salt solution (DSS) to induce intestinal sloughing and colitis, these mice exhibited a diminished population of Tregs and more severe colitis with increased levels of pro-inflammatory type cytokines compared to the wild type mice (Fluck et al. 2015).

Obese individuals have low-grade chronic inflammation which reduces wound healing and makes them more prone to having inflammation in barrier tissues (Blakytny and Jude 2006, Hass et al. 2006, Steed et al. 2009, Farah et al. 2011). Our laboratory and others have shown that epithelial barrier integrity becomes compromised in obesity. Obesity causes elevated inflammation that overstimulates and decreases the number of T cells locally in the epithelial layer of the skin. This inflammation reduces T cells growth factor production that normally helps with the proliferation of fibroblasts, keratinocytes, and endothelial cells (Taylor et al. 2010, Clark et al. 2005 Kern et al. 2001, Halle et al. 2004, Seitz et al. 2010, Park et al. 2010, Petermann et al. 2010, Brandes et al. 2003, Eberl et al. 2009, Komori et al. 2012). This reduction in T cell number and function leads to a disruption in keratinocyte homeostasis and normal barrier tissue function in the skin (Taylor et al. 2010).

Obesity impacts the intestinal barrier tissue

Obese patients have a more severe form of two major inflammatory bowel diseases: Crohn's disease and ulcerative colitis (Steed et al. 2009, Hass et al. 2006). Subjects suffering from obesity compared to non-obese patients experience a more active form of Crohn's disease, where symptoms develop quicker and are more severe (Steed et al. 2009, Hass et al. 2006).

Increased leptin levels found in obese patients correlate with an increased probability of developing colorectal cancer (Koda et al. 2007).

Patients suffering from inflammatory bowel disease alone, experience an increased number of systemic γδ T cells in the blood (Giacomelli et al. 1994) and a rise in intestinal mucosal γδ T cells at the sites of inflammation which may contribute to the overall inflammatory immune disorder (McVay et al. 1997, Yeung et al. 2000). The mucosal γδ T cells that were isolated from the inflammatory sites were shown to be a major source of IFN-γ cytokine production (McVay et al. 1997). It is still unknown what effects systemic inflammation, caused by obesity, have on the population of γδ intraepithelial intestinal lymphocytes and their functionality.

Mouse models of obesity display changes in the gut barrier tissue. Mice that are *ob/ob* (leptin deficient mice) and *db/db* (leptin receptor deficient mice) exhibit tight junction gaps leading to increased permeability in the intestinal tissue (Brun et al. 2006, Cani et al. 2006). This increased permeability can cause an increase in bacterial translocation from the mucosal epithelium to the lamina propria, which can increase local inflammation (Brun et al. 2006).

Intestinal T lymphocyte populations

Mammals have evolved villi or folds in the walls of the intestine to increase intestinal surface area and maximize their ability for absorption. In the epithelial layer of the villi reside intraepithelial intestinal lymphocytes that maintain epithelial homeostasis, repair damaged intestinal tissue, and fight off enteric pathogens (**Figure 1**) (Cheroutre et al. 2011).

Intestinal intraepithelial lymphocytes (IELs) are CD3+ T cell precursors that originate in the bone marrow, develop in the thymus, and differentiate into 'natural' or 'induced' IELs (Hayday and Gibbons 2008, Cherourtre et al.2011). Natural IELs develop and differentiate in the thymus while the induced IELs are established after conventional T cells seed into intestine and recognize the MHC Class I and MHC Class II peptide antigens post-thymically (Cherourtre et al. 2011). Natural IELs express either TCRγδ or TCRαβ and are either negative for both CD4 and CD8 (CD4-/CD8-) or express CD8αα (Jarry et al. 1990, Hayday and Gibbons 2008) (**Table 1**). Induced IELs all express TCRαβ along with either CD8αβ+, CD4+, or CD4+ and CD8αα+ (**Table 1**) (Hayday and Gibbons 2008). γδ or αβ receptor expressing T cells develop in the thymus from the 18th day of embryonic development until 28 days following birth (Leandersson et al. 2006, Cheroutre and Lambolez 2008, Havran and Allison 1988, Havran and Allison 1990 Gagadharn et al. 2006, Pennington et al. 2003).

The mature T cells migrate and seed in the intestinal epidermis between 2 and 4 weeks of age in mice. Once seeded, the immune cells differentiate and proliferate to protect the barrier tissue (Havran and Allison 1988, Ito et al. 1989). T cells develop at different stages of life, and disruptions of T cell development can possibly alter their number and function. It is established that the CD3+ T cells found in gut epithelium express different T cell receptors (Vγ7, Vγ4, Vγ5) compared to the peripheral blood (Vγ1), lung (Vγ2), and skin (Vγ3) (Jarry et al. 1990, Girardi 2006).

T lymphocyte function in the intestine

The good

Intestinal γδ T cells densely populate the intestinal epithelia, composing 60% of all intestinal intraepithelial lymphocytes (Darlinton et al. 1996, Bonneville et al 1998). γδ T cells in the intestines have a distinct Vγ/Vδ chain and it is also referred to as Vγ5+ (Giradi 2006, Cheroutre et al. 2011). γδ T cells produce growth factors and cytokines that regulate the homeostasis of the intestine, and interact with other immune cells in the barrier tissue (Boismenu et al. 1994). Upon activation, γδ T cells produce keratinoctye growth factor-1 (KGF-1) and transforming growth factor- beta (TGF-β) that help initiate epithelial proliferation and repair damage to the intestinal wall (Boismenu and Havran 1994, Inagaki-Ohar et al. 2004). During periods of infection, γδ T cells demonstrate antimicrobial properties and produce IFN-γ to protect against bacterial infections such as *Listeria monocytogens* and reduce the severity of colitis compared to the mice deficient for γδ T cells (Hamada et al. 2008, Kuhl et al. 2007, Chen et al. 2002). Intestinal γδ T cells maintain the integrity of epithelial tight junctions during an infection (Dalton et al. 2006, Roberts et al. 1996). γδ T cells are also necessary to control susceptibility against parasitic infections such as Toxoplasma gondii (Egan et al. 2005).

Our laboratory is interested in understanding the mechanisms used by γδ T cells in tissue repair of the intestine. γδ T cell deficient mice have impaired barrier function and delayed tissue repair (Jameson et al. 2004, Jameson et al. 2002, Toulon et al. 2009). A mouse model of IBD has been established by treating mice with dextran sulfate sodium (DSS) salt solution in their drinking water to induce colitis and lesions in the colon. Using this model, wild type mice and TCRαβ deficient mice (TCRα-/-) experience colitis, which improves upon removing DSS from the water. However, γδ TCR deficient mice (TCRδ-/-) have a reduced ability to recover from DSS induced colitis, resulting in an increase in mortality among TCRδ-/- mice (Chen et al. 2002). These studies suggest that γδ IEL support, repair and defend against pathogens during

DSS induced colitis. As mentioned previously, when the intestine is damaged, the γδ IEL release cytokines KGF-1 and TGF-β at the wound site to help with epithelial repair (Boismenu et al. 1996, Chen et al. 2002, Montufar-Solis et al. 2007). In addition, KGF-1 deficient mice were shown to have increased mortality during the DSS induced colitis treatment suggesting that γδ-produced KGF-1 is the major factor required for intestinal epithelial repair in colitis (Chen et al. 2002).

Beyond γδ T cells, there are a variety of αβ T cells in the intestine that have distinct protective roles. One population is identified by CD8αα and αβ TCR expression. These T cells have a cytotoxic phenotype and differentiate in response to self-antigens to destroy malignant and stressed epithelial cells (Gagadharan et al. 2006). Another population of T cells expresses CD8αβ and αβ TCR receptors. These T cells defend against viral and parasitic infections like the simian immunodeficiency virus, choriomeningitis virus, rotavirus, *Toxoplasma gondii,* and *Giardia lamblia* (Hansen et al. 2009, Muller et al. 2000, Dharakul et al.1991, Lepage et al. 1998, Kanwar et al.1986). A third population of T cells in the intestine express the CD4+ and αβ TCR receptors. Importantly, these T cells maintain tissue integrity and control translocation of enteric bacteria in the intestines (Mehandru et al. 2004, Li et al. 2005, Epple et al. 2010). Furthermore, CD4+ T cells regulate the response and infection of extracellular microbial pathogens such as *Salmonella typhimurium* (Dandekar et al. 2010). During chronic stimulation, CD4+ Tregs control inflammation by suppressing the immune response and collaborate with CD4+ T cells to make IL-10 which is an anti-inflammatory cytokine (Park et al. 2010). Intestinal T cells play an important role in facilitating protective responses against infection, however these same cells can also produce negative responses under inflammatory conditions.

The bad

γδ T cells produce inflammatory cytokines when the epidermal layer of the intestine is damaged and or becomes infected. γδ T cells are known to play a pro-inflammatory role in inflammatory bowel disease and can actually exacerbate the disease. In inflamed intestinal tissue, γδ T cells produce increased levels of IL-17 cytokine, which has been shown to aggravate colitis (Park et al. 2010). Interestingly, αβ T cell deficient mice (TCRα-/-) have been shown to develop spontaneous colitis (Mizoguchi et al. 1996). This may be due to the absence of CD4+ Treg and the presence of pro-inflammatory γδ T cells. The balance between these cellular populations seems to be critical for intestinal homeostasis.

Intraepithelial lymphocytes are known to generate inflammatory conditions. CD8αβ+TCRαβ+ T cells are also shown to initiate autoimmune colitis by increasing IL-17 production and by exacerbating coeliac disease by the Natural Killer group 2, member D (NKG2D) signaling pathway (Tajima et al. 2008, Meresse et al. 2004, Hue et al. 2004). In addition, patients with coeliac disease have active CD4+ TCRαβ+ T cells that produce higher amounts of IFN-γ which further induces small intestine inflammation (Van Wijk and Cheroutre 2010). The elevated amounts of IL-15 and IFN-α proinflammatory cytokines are also thought to stimulate the differentiation of pathogenic CD4+ T cells. Intestinal T cells that are overstimulated under inflammatory conditions can end up being more harmful than helpful when their homeostatic environment is altered. Although we know that changes to the T cell homeostatic environment will alter T cell development, it is unknown if the inflammatory conditions caused by obesity will contribute to intraepithelial lymphocyte reduction and dysfunction by overstimulation of their receptors.

The gap

T cells assist in immune responses and it has been accepted that obese individuals have delayed tissue repair at least partially due to reduced T cell number and function in the skin (Cheung et al. 2012, Taylor et al. 2010). However, not much is known about how intestinal intraepithelial lymphocyte populations are affected by the metabolic disease of obesity. Furthermore, there are no studies that compare the maturation stages at the onset of obesity. Little is known regarding how intestinal disease severity and tissue repair complications in obese children compare with those in the intestines of obese adults, and no available studies exist in mice. The proposed experiments will explore whether or not the maturation stage at the onset of obesity compromises intraepithelial lymphocyte number and function. Once we understand how intestinal lymphocytes are impacted by obesity we can identify whether they would be good targets for therapeutics to treat IBD in obese children and adults.

Here, we study the effect of obesity onset on intestinal intraepithelial lymphocytes. For this purpose, we utilized a well-studied mouse model of diet-induced obesity. Lin et al. placed 3 week old mice on a similar composition of HFD and NCD and measured body weight, energy intake, adipose tissue mass, and plasma leptin (Lin et al. 2000). The mice were fed a HFD (containing 58% fat, 14% carbohydrate and 27.3% protein) or a NCD (containing 9.7% fat, 63% carbohydrate and 27% protein) for 1 week, 8 weeks, 15 weeks, or 19 weeks. The authors categorized different stages of HFD induced obesity as early (1 week), middle (8 weeks) and late stage of obesity (after 19 weeks) by comparing body weight, fat gain, energy intake, and leptin resistance. They showed that during the early stage of HFD induced obesity, mice exhibited elevated body weight, fat storage but normal food intake. They also showed that mice on different diets starting from the second week showed significant changes in body weight (Lin et

al. 2000). The longer the mice are on the HFD, the greater the increase in body weight, fat gain, energy intake, and greater the resistance to leptin. Many studies have placed mice on a HFD for 12-52 weeks which is generally considered to be the middle to late stages of obesity. For example, Xue et al. and Yang et al. investigated how late stage obesity affects inflammation, and insulin resistance, and T cell receptor repertoire diversity in adipose tissue (Xu et al. 2003, Yang et al. 2010). In our study, we investigate how the middle stage of HFD induced obesity affects IELs.

We fed mice a HFD for 7 weeks starting at different maturation stages to provide preliminary data that can be compared to childhood, adolescent, and adult onset of obesity in humans. To define the stages of maturation we utilized data from previously published studies. At 3 weeks of age, mice are weaned from their parents and are able to consume pellet food and drink on their own (Jackson and Abbot 2000, Dutta and Sengupta 2016). In humans, weaning is when the infant transitions from breast feeding or bottle nursing to eating other food (Paediatrics & Child Health 2004). Thus, we studied weanling mice at 3 weeks of age as a comparison to human infants. At 6 weeks old, mice start to regulate gonadotropin levels and increase sex steroids in body (Nelson et al. 1990). Female mice start to have vaginal cornifation while the male mice have blano-reputial separation (Nelson et al. 1990). Humans start puberty or are considered adolescents around 11.5 years (Artnett 2012). Thus, we studied adolescent mice at 6 weeks of age. At 10 weeks of age, mice are sexually mature (Jackson and Abbot 2000). In humans, adults have growth plate closure unlike adolescents who are still developing (Rogol et al. 2002). Thus, we studied adult mice starting at 10 weeks of age.

Objective and hypothesis

This study investigates how weanling, adolescent, or adult onset of obesity impacts intestinal intraepithelial lymphocyte seeding, homeostasis, and function. Previous studies have shown that adult obesity impairs function and decreases the quantity of skin epidermal γδ T cells, which leaves the skin vulnerable to chronic wounds and infections (Taylor et al. 2010, Taylor et al. 2011). We predict that mice whose obesity onset begins while they are weanlings will experience greater complications related to changes in T cell populations than mice whose obesity begins later, in adulthood. To evaluate this hypothesis, we measured T cell numbers and cytokine functions for mice at three different stages of maturity (weanling, adolescent, and adult). We speculate that γδ T cells will have difficulty proliferating in the intestinal epithelium due to the chronic low-grade pro-inflammatory obese environment. This research will help us further understand the metabolic disease of obesity in order to identify mechanisms that could restore intraepithelial lymphocyte number and function and promote intestinal homeostasis and barrier function.

Preliminary Results

Our previous data (currently being submitted for publication) shows that obesity starting in adolescent mice results in epithelial barrier tissue dysfunction in the small intestine and colon. 6 week-old adolescent wild-type C57BL/6J male mice were placed on a normal control diet, 17 kcal% fat diet (Teklad LM-485, Harlan Laboratory), or HFD, 60 kcal% fat diet (D12492, Research Diets) for at least 14 weeks (**Table 2**). Mice on the HFD experienced epidermal T cell loss in the proximal, medial, and distal sections of the small intestine (**Figure 4A, 4B)** Fluorescent staining confirms that CD3+, γδ, and αβ T cells are reduced in the intestinal epithelium but their αβ to γδ T cell proportions remain similar (**Figure 5A, 5B)**.

Materials and methods

Ethics statement

All animals were handled in the vivarium at CSUSM in strict accordance with good animal practice as defined by the relevant national and/or local animal welfare bodies (IACUC #12-014).

Mice

Wild-type C57BL/6N male mice were purchased from Taconic Farms Inc. (New York) and housed and bred at the vivarium in California State University of San Marcos. The facility uses a 14 hour light and 10 hour dark cycle daily. Four mice per cage were given ad libitum access to food and water. For obesity experiments, wild-type male C57BL/6N mice were placed on a HFD which is a 60 kcal% fat diet (Research Diets, D12492) starting at 3, 6, or 10 weeks of age, and control age-matched male mice were maintained on a NCD 17 kcal% fat diet (Harlan Laboratory, Teklad LM-485) (**Table 2, 4**). All mice were weighed weekly. The NCD and HFD were refreshed once weekly and the cages were changed every other week.

Mouse model

Little is known about how the age of obesity onset affects intestinal intraepithelial lymphocytes. To investigate the maturation stage of obesity onset, we examined a well-studied murine model of obesity using a 60 kcal% high fat diet, which we initiated at different ages (**Table 4**) (Buettner 2007). In this study we categorize the different age groups as ”weanling”, “adolescent”, or ”adult” as per the maturation stages occurring and these form the different cohorts of our study. We define the baseline age for classification as follows: “weanling” starting

at 3 weeks, “adolescent” starting at 6 weeks and “adult” starting at 10 weeks. These three cohorts were administered high fat diet for 7 weeks in order to study the effect of maturation stage on the onset of diet-induced obesity (Dutta and Sengupta 2016, Fox et al. 2007, Rooney et al. 2010) (**Table 3 and 4**). 19-42 mice were studied for each age cohort with 9-21 mice per diet, for a total of 85. Mice were weighed weekly to assess weight gain. A HFD was administered for 7 weeks because our preliminary data has shown that 7 weeks on a high fat diet is sufficient to observe reduced T cell numbers in the intestine. Food, water, and calorie consumption were calculated weekly from 10-20 mice in each age cohort, with 4-10 mice per diet, for a total of 36 mice. Estimated grams and percentage of total fat mass were calculated by measuring the mouse wet mass and the dried mass after incubating the mouse carcasses at 58°C for two weeks. The weights were inputted into this equation for estimated fat proportion: Y=1.0844x-0.2818, x= dry mass/wet mass (Hasting and Hill 1989, Dr. Kristan).

Small intestine immunofluorescent staining

The small intestine was isolated, cut into 3 equal sections and labeled as proximal, middle, and distal portions of the intestine. The proximal section is located closest to the stomach and the distal portion is closest to the cecum. The different sections were embedded into a “Swiss roll” in optimum cutting temperature (O.C.T.) compound (Tissue-Tek, 14-373-65), and stored at -80^{o}C (**Figure 2**). The proximal frozen sections were cut into 8 µm thick sections using a cryostat. Sections were fixed with 4% methanol free formaldehyde (Polysciences Inc., 04018) for 10 minutes, incubated in a gelatin block for 30 minutes [Gelatin Block composition: 2.5% Goat Serum (Gibco, Life Technologies, 16210-064), 2.5% Donkey Serum (Sigma-Aldrich, D9663), 1% Bovine Serum Albumin Essential Fatty Acid Free (Sigma-Aldrich, A6003), 2.0%

Gelatin From Cold Water Fish Skin (Sigma-Aldrich, G7765), 0.1% Triton X-100 (Sigma-Aldrich, X100), 0.3 grams of Glycine (Sigma-Aldrich, G7126), 82% Dulbecco's Phosphate-Buffered Saline Without Calcium & Magnesium (Corning Cellgro, 21-031-CM)]. Next, samples were immunostained with 10 µg/ml of CD3+PE antibody (Biolegend, 145-2C11) in Dulbecco's Phosphate-Buffered Saline without Calcium & Magnesium (Corning Cellgro, 21-031-CM) to detect T cell populations. Sections were mounted with SlowFade Gold Antifade Mounting media with DAPI (Life Technologies, S36939) to counter-stain the cell nuclei. Digital images at 20x magnification were acquired using an immunofluorescent microscope (Nikon, Microphot-FXL) and Nikon camera (Nikon, DS-Fi1c). Images were merged together using Adobe Photoshop CS6 software, and analyzed using ImageJ software (NIH). Mean values of epithelial T cells per millimeter of villi length ± standard deviation were calculated. More than 35 images of small intestine were acquired and analyzed per mouse. The average number of T cells per mm of intestinal epithelia was calculated per mouse using 4-16 mice in each age cohort, with 4-6 mice per diet, for a total of 46 mice.

Intestinal intraepithelial cell preparation

Intestinal epithelial cells were isolated from the whole small intestine tissue of mice by first removing the Peyer's patches and cutting the small intestine to approximately 5-mm in length. The pieces were rinsed in RPMI (Corning Cellgro, 10-1017-CV) and DTT (Sigma, D5545), to remove the mucus, and then suspended in 1x Hank's Balanced Salt Solution without Calcium and Magnesium (Gibco, 14185052), 25mM HEPES (Gibco, 156630080), 1mM DTT (Sigma, D5545), 1mM EDTA (Life Technology, 15575020), and 10% heat-inactivated FBS (Omega, FB-01) solution. The supernatant was filtered through a 70µm cell strainer and added to

Percoll (Sigma, P1644) to produce a 40% Percoll solution. This 40% Percoll solution was then overlaid on a 70% Percoll solution producing a gradient. The cells in the buffered layer between the 40% and 70% Percoll layers were then collected. The isolated cells were stained with antibodies for flow cytometric analysis (**Figure 3A, 3B, 3C, Table 5**). For *in vitro* stimulation, the intestinal epithelial cells were placed into RPMI complete media, which consists of RPMI (Corning Cellgro, 10-1017-CV), with 10% heat-inactivated FBS (Omega, FB-01), 10 U/ml recombinant IL-2 (NCI, 9703031), 25mM HEPES (Gibco, 156630080), 1x MEM NEAA (Gibco, 1140-050), 1mM Sodium Pyruvate (Gibco, 11360-070), 1x Pen Strep Glutamine (Gibco, 10378), 0.05mM 2-Mercaptoethanol (Sigma, 60-24-2). In this solution, the cells were stimulated 5 hours with or without PMA (EMD Millipore Corporation, 524400) and Ionomycin (Calbiochem,407950). Approximately 1 hours after culturing, 20ug/ml Brefeldin A (Sigma, B7651) was added for 4 hours at 37ºC to block protein transport in order to look at the accumulation of intracellular cytokines. Next, the intestinal epithelial cells were stained with antibodies and fixed with 1% folmaldehyde for flow cytometric analysis (**Table 5).** Intracellular cytokine staining and fixing were performed using the BD Cytofix/Cytoperm kit (BD Biosciences) per manufacturer's instructions. Cells were then stored at 4 ºC and analyzed by flow cytometry. All cells were centrifuged using a Sorvall RT7 centrifuge at 1,500 rpm at 4ºC and cultured at 37ºC with 5% CO_2 and atmospheric (20%) oxygen.

Flow cytometry staining

The following antibodies were used: FITC-, PE-, PerCP/Cy5.5, or APC CD3+ (Biolegend, 145-2C11), CD4 (Biolegend, GK1.5), CD8α (Biolegend, 53-6.7), αβ TCR(Biolegend, H57-597), γδ TCR (Biolegend,GL3), TNF-α (Biolegend, MP6XT22), and IFN-

γ (Biolegend, XMG1.2). Surface receptors were stained using 0.5 µg/ml antibody solutions in 1x Dulbecco's Phosphate-Buffered Saline without Calcium & Magnesium (Corning Cellgro, 21-031-CM) containing 2% heat-inactivated FBS (Omega, FB-01) and 0.2% NaN_3 for 20 min at 4°C. Intracellular cytokine staining and fixing were performed using BD Cytofix/Cytoperm kit (BD Biosciences, 554714) per the manufacturer's directions.

T cells were acquired and quantified using BD Accuri C6 software on Accuri C6 (BD Biosciences) and analyzed with FlowJo software (Tree Star, Inc.). For flow cytometry plots, gating was determined for each individual experiment using negative unstained and positive compensation controls (**Figure 3A, 3B, 3C, Table 5**). The average number and percentage of each specific live T cell population was compared between the mice on different diets, for each age cohort. 8-14 mice were used in each age cohort, with 4-9 mice per diet, for a total of 33 mice.

Data analysis/statistics

Body mass, food intake, calorie intake, water intake were analyzed with repeated measures analysis of variance (ANOVA) on Prism (GraphPad) using "mice on different diets" (Normal chow diet, High fat diet) as the between subjects factors, and "days of experiment" as the within subject factor.

T cell numbers and cytokine levels from sacrificed mice at the end of the 7 week period on the normal chow diet and the high fat diet were statistically analyzed using two-way ANOVA using "mice on different diets" (Normal chow diet, High fat diet) as the row factor and the "different cohorts of mice" (Weanling, Adolescent, and Adult) as the column factor using Prism (GraphPad) software. Cytokine producing T cells were calculated by subtracting the value of

stimulated cells by value of unstimulated cells. Results were considered significant with a P value <0.05.

Results

Weanling, adolescent, and adult mouse cohorts all have significant weight gain after 7 weeks of consuming a HFD.

To examine if mice fed a 60 kcal% fat diet (HFD) at different stages of maturation gain a significant amount of body weight, mice starting at 3, 6, or 10 weeks of age received a HFD or NCD for 7 weeks. The body weight and body composition of the mice were analyzed.

Weanling mice administered a HFD gained significantly more body weight within 3 weeks as compared to their weanling NCD fed counterparts **(Figure 6A)**. The HFD mice in this cohort overall consumed significantly less food **(Figure 6B)** and water **(Figure 6D)** during the 7 week diet. The Calorie intake was similar throughout the study although there was a slight increase in Calorie consumption during the 3rd week and 4th week in the HFD fed mice as compared to the NCD fed controls **(Figure 6C).**

Adolescent mice placed on a HFD gained significantly more weight within 2 weeks as compared to their NCD fed counterparts **(Figure 7A).** The mice on a HFD ate significantly less food **(Figure 7B)** and drank significantly less water **(Figure 7D)** throughout the study. The Calorie intake was similar in the both the HFD and NCD fed mice after the 1st week of the treatment (**Figure 7C).**

Adult mice fed a HFD gained significantly more weight within 2 weeks as compared to their NCD fed counterparts **(Figure 8A)**. While the mice fed a HFD gained weight during the study, the NCD fed mice did not exhibit significant weight gain. The HFD fed mice ate significantly less food **(Figure 8B)** after week 4 and drank less water throughout **(Figure 8D)**.

The Calorie intake was similar between the groups except during the 1st and 6th weeks of treatment **(Figure 8C).**

In all three cohorts, mice fed a HFD gained more weight as compared to the NCD fed mice **(Figure 9A, 9B)**. Moreover, among the different cohorts, given that all cohorts were examined for the same duration of 7 weeks, the weanling mice gained the most weight (**Figure 9C, 9D)**. The adult mice gained the least amount of weight likely due to the fact that they started at almost full size (**Figure 9C, 9D)**.

To further characterize whether 7 weeks of HFD induced obesity, body composition was analyzed by quantifying fat mass and total fat percentage from weanling, adolescent, and adult cohort of mice. All mice administered a HFD had a significant increase of fat mass compared to the mice administered a NCD. The adult mice gained the most amount of fat mass as compared to weanling and adolescent cohorts from the start of the study **(Figure 10A, 10B)**. In addition, the percentage of total fat in the cohorts of HFD fed mice was significantly more than the NCD fed mice. Much the same way as the gain in fat mass, the percentage of total fat in the adult mice on HFD is higher than the other cohorts on HFD. **(Figure 10C, 10D)**. Interestingly, among the different cohorts, mice fed continually on NCD had no gain in fat mass or change in percentage of total mass over time (Figure 10). Since all cohorts of mice on a HFD exhibited at least an increase of 20% of their original body weight and over 30% of their body composition as fat mass, administration of a HFD for 7 weeks did induce obesity.

Obese mice exhibit significantly lower numbers of T cells in the intestinal epithelium in all cohorts with weanling mice on a HFD exhibiting the lowest number of intestinal epithelial T cells.

To identify whether obesity has a detrimental effect on intestinal intraepithelial lymphocyte number, we performed immunofluorescent staining of intestinal sections to detect CD3+ T cells which reside in the epithelial layer of the small intestine. Importantly, CD3+ T cells were reduced in HFD fed mice compared to the NCD fed mice in all three cohorts **(Figure 11, 12, Table 6).**

At 3 weeks of age (*weanling* baseline) weanling mice have an average of 3 T cells/mm **(Figure 11A, 12A, Table 6).** When these 3 week old mice were placed on a 7 week NCD, at the end of the treatment there was an average of 12 T cells/mm. However, when 3 week old mice were placed on a HFD for 7 weeks, the mice fed a HFD had an average of 4 T cells/mm at the end of the treatment. This was similar to the 3 week old weanling mice. This shows that administering a HFD during the weaning stage is detrimental to IEL numbers. This may be due to impaired proliferation of the T cells that seed the intestine and/or to reduced migration of T cells to the intestine. In either case, the T cells are not able to reach their full potential number.

When mice are 6 weeks of age (*adolescent* baseline), adolescent mice have an average of 12 T cells/mm. In our experiment, this was similar to the 3 week old mice fed a 7 week NCD (**Figure 11B, 12B, Table 6**). When 6 week old mice were fed a NCD for 7 weeks, there was an overall increase in the number of CD3+ IELs to 22 T cells/mm. In contrast, when 6 week old mice were placed on a HFD for 7 weeks, on average there were 10 T cells/mm. This is even lower than the number of CD3+ T cells in the 6 week adolescent baseline mice. Again, this

suggests that CD3+ T cells are unable to proliferate and/or migrate to the intestine during HFD administration.

When mice are 10 weeks of age (*adult* baseline), adult mice have an average of 13 T cells/mm. In our experiment, this was similar to the 6 week old, adolescent baseline mice (**Figure 11C, 12C, Table 6)**. Furthermore, as expected, this was similar to the 3 week old mice placed on a 7 week NCD. NCD given to the 10 week old adult mice for 7 weeks resulted in an average of 20 T cells/mm. This suggests that the IELs reach their full IEL number between 10-17 weeks of age since 20-30 week old mice exhibit an average of 22 T cells/mm (Figure 4). However, when 10 week old adult mice were fed a HFD for 7 weeks, not only did these mice have reduced CD3+ IELs (10 T cells/mm) compared to the NCD, but they were reduced further than the adult baseline.

We hypothesized that childhood obesity (*weanling* cohort) would be more detrimental than the adolescent and adult onset obesity. Our data shows that after HFD administration, obese mice belonging to the weanling cohort had a 65% reduction in T cells/mm as compared to NCD fed non-obese mice. When compared between the three cohorts i.e, weanling, adolescent, and adult, this reduction in the IELs of the weanling HFD fed mice was the greatest (**Table 6**). When the T cells/mm was normalized to the baseline, the weanling mice that were placed on a NCD had a 4.5-fold increase in T cells/mm. In contrast, the weanling mice placed on a HFD for the same duration of time had a 1.6-fold increase in T cells/mm. This suggests that HFD administration causes a decline in the number of IELs or prevents the accumulation of IELs during maturation.

The obese *adolescent* mice had a 55% reduction in T cells/mm as compared to NCD fed mice (**Table 6**). When the T cells number/mm was normalized to the baseline, the NCD fed mice

had a 1.9-fold increase and the HFD fed mice had a 0.9-fold change. This shows that the adolescent mice administered a HFD have fewer IELs /mm as compared to the start of the new diet.

The *adult* mice fed a HFD had a 50% reduction in T cells/mm as compared to NCD fed mice (**Table 6**). When the IEL number/mm was normalized to the baseline, the NCD fed mice had a 1.5-fold increase and the adult HFD fed mice had a 0.8-fold change. Again, administration of a HFD reduced the IEL number below the original baseline for the adult cohort.

These histology results show that obesity at any age is detrimental to the IEL population, and obesity can have different effects on IEL population depending on the age of onset. This finding was also supported by flow cytometry. IEL were isolated from the small intestine and examined by flow cytometry. The isolated cells were first gated on live lymphocyte then further gated on CD3+ T cells. The weanling mice on a HFD had significantly less live lymphocytes compared to the weanling mice on a NCD, which shows that the cells are more sensitive or fragile to the T cell isolation process compared to the adolescent or adult mice (**Figure 13A, 13B**). The CD3+ live-gated T cells were significantly reduced in the HFD administered weanling and adolescent cohorts (**Figure 13C**) as compared to the mice fed a NCD. However, when examining the absolute number of CD3+ T cells, they were only significantly reduced in the weanling cohort of mice (**Figure 13D**).

Obesity reduces γδ T cell number in the intestinal epithelium of all three cohorts of mice, and skews T cells away from a CD8α-expressing phenotype in adolescent and adult mice.

The live CD3+ T cell population was further analyzed to determine the γδ T cell percentage and number. In agreement with previous results from our laboratory, there was no

significant change in γδ T cell percentages between a HFD and the NCD administered mice from weanling, adolescent and adult cohort (**Figure 5A, 14A**). This suggests that both αβ and γδ T cells are equally reduced in mice administered a HFD. Similar to the histology findings with CD3+ T cells, the number of γδ T cells was significantly reduced in the HFD fed mice compared to the NCD fed mice from all three cohorts (**Figure 14B**). When these γδ T cells were further gated using CD8α, HFD fed adolescent and adult cohorts were less skewed towards the CD8α phenotype (**Figure 14C**).

Obesity does not change αβ T cells percentage or number but skews these αβ T cells toward a CD4+ phenotype in the adolescent cohort.

The αβ T cell percentage and number were also quantified from the CD3+ T cell population in all three cohorts of mice. There was no significant change in αβ T cell percentage between the NCD and HFD mice (**Figure 15A**). This shows that γδ and αβ are equally represented and neither population is selectively lost. However, they can be equally lost. Although not significant, in 9 out of 12 experiments there was a reduction in αβ T cell number in the HFD weanling mice compared to the NCD fed controls (**Figure 15B**). When the αβ T cells were further examined, there was a significant increase in αβ T cells skewing toward a CD4+ phenotype in the HFD fed adolescent mice compared to the control (**Figure 15C**).

Obese adolescent and adult mice had increased amounts of γδ T cells that express proinflammatory type cytokine, TNF-α.

To determine if the remaining intraepithelial T cells are functional in obese mice, we isolated intraepithelial T cells from the intestine of weanling, adolescent, and adult obese mice

and compared them to lean control mice. Isolated IELs were stimulated with Concanavalin A to evaluate TNF-α and IFN-γ cytokine production. These cytokines are key factors involved in the regulation of infection and wound repair (Potten et al. 1995, Chen et al. 2002, Hahm et al. 2001). We hypothesized that there would be a reduction in the number of T cells expressing cytokine by these T cells in obese mice from all three cohorts as compared to their lean counterparts. In addition, we hypothesized that the T cells in the intestine would be more sensitive to weanling obesity and thus exhibit a more dramatic reduction in function. Weanlings have a limited population of intestinal T cells to start with due to the fact that their immune cells have not fully developed and proliferated. Therefore, any alteration to the intestinal environment may adversely affect their development and function.

Overall, the weanling mice fed a HFD exhibited similar number of cells positive for TNF-α as the mice fed a NCD in all T cell populations examined (**Figure 16, 17**). On the other hand, the HFD fed adolescent and adult mice exhibited significant increase in TNF-α producing cells compared to NCD-fed controls.

For a more detailed analysis, the T cells were broken down into distinct populations of αβ/γδ TCR expression and CD4/CD8 expression. The CD3+ T cell population in HFD fed adolescent mice had an increase in TNF-α producing cells compared to their NCD control (**Figure 16A**). Within the CD3+ T cell population, the γδ CD8α+ T cells had a significant increase in TNF-α production when mice were fed a HFD compared to NCD. CD8α+ T cells in adolescent mice also had a significant increase in TNF-α production compared to the CD8α+ T cells from weanling mice fed a HFD (**Figure 16C**). Within the αβ T cell population, the mice fed a HFD had greater amount of CD4+ T cells producing TNF-α compared to NCD fed mice, in 3 of 4 experiments, although this data is not significant (**Figure 17**).

In the adult mice fed a HFD, although not significant, there was a modest increase in CD3+ T cells producing TNF-α, in 3 of 4 experiments. (**Figure 16A**) Within this CD3+ T cell population, significantly more γδ T cells produced TNF-α when these mice were fed a HFD compared to the NCD (**Figure 16B**). There was an increase of γδ T cells that produce TNF-α in the adult as compared to the weaned when both were fed a HFD. Within this γδ T cell population, the CD8α+ T cells produced more TNF-α when adult mice were fed a HFD compared to NCD. Moreover, CD8α+ T cells producing TNF-α was also increased in adult mice compared to weanling mice, both on a HFD (**Figure 16C**). Furthermore, αβ T cells in the adult HFD mice had an increase in number of cells producing TNF-α in 3 of 4 experiments, although this is not significant. Within the αβ T cell population, significantly more CD4+ T cells produced TNF-α in the HFD fed adult mice compared to their lean control (**Figure 17B**).

No statistical change in IFN-γ production by γδ T cells from weanling, adolescent or adult cohorts. Obesity results in reduced IFN-γ production by CD4+ T cells in adult mice.

Although not significant, the weanling mice fed a HFD exhibited fewer T cells producing IFN-γ compared to the control in 3 of 4 experiments (**Figure 18A**). Within the CD3+ T cells, αβ T cells had reduced number of IFN-γ producing cells in the HFD fed mice compared to the NCD fed mice (**Figure 19A**). In all four experiments performed in the weanling mice, the HFD fed mice had fewer IFN-γ producing T cells.

In the adolescent cohort, the HFD fed mice do not have significant changes in IFN-γ production in the CD3+ T cells, αβ, γδ, CD4+, and CD8α+ T cell populations (**Figure 18, 19**). Similarly, in the HFD fed adult cohort the mice do not have significant changes in IFN-γ producing CD3+ T cells, αβ, γδ, and CD8α+ T cell populations (**Figure 18, 19**). However, HFD

fed adult mice exhibit more CD4+ T cells producing IFN-γ compared to the NCD control (**Figure 19B**). There is also a significant increase in IFN-γ producing cells between the NCD adult and the NCD adolescent mouse cohorts (**Figure 19B**) Overall, the IFN-γ trend between the NCD and HFD fed mice in the weanling cohort is different from the adolescent and adult cohort of mice. This trend can potentially be interesting. However, we would have to perform more experiments to establish this finding.

Discussion

To investigate how the age of obesity onset affects intestinal intraepithelial lymphocytes, we placed mice at different maturation states (weanling, adolescent, and adult) on a NCD or a HFD for 7 weeks. We compared body weight and fat mass from these cohorts of mice. The adolescent and adult mice on a NCD only had a marginal weight gain. This is likely due to weanling mice growing at a faster rate, while the adolescent and adult mice have reached a limit to their weight gain. The same differences were noted when the cohorts were fed a HFD. In all three cohorts of mice, placing the mice on a HFD increased body mass and adipose fat tissue. Therefore, the HFD was shown to cause diet induced obesity in all three cohorts of mice.

There are at least two mechanisms that may account for the lack of T cells in weanling mice fed a HFD. The first possibility is that the IELs proliferate for a short period of time but then become reduced in number. This reduction might be due to the IELs migrating out of the epithelial layer of the small intestine or undergoing apoptosis (Park et al, manuscript submitted). IELs have CCR9 and CD103 which are a chemokine and adhesion receptors, respectively, that help the cells home to the epithelial layer of the intestine (Ericsson et al. 2004, Uehara et al. 2004, Schon et al. 1999, Edelblum et al. 2009). Our previous data, show that IELs isolated from HFD fed mice have reduced expression of CCR9 and CD103 (Park et al, manuscript submitted). The second possibility is that the IELs could not migrate to the intestine and proliferate to maintain homeostatic IEL numbers, all of which is ongoing at that age (Havran and Allison 1988, Ito et al. 1989). In this case, obesity may impair the ability of the IELs to seed the intestinal niche. However, further studies are needed to investigate which of these hypotheses is correct.

Our immunohistology data reveals the period when IELs reach their full IEL number and to what extent HFD induced obesity can reduce IEL persistence in the intestine. We identified that at 10-17 weeks of age, IELs had filled the intestinal epithelial compartment. When adolescent or adult mice were placed on a HFD, there was a reduction of the IEL number compared to the NCD fed mice. The mechanism may be that the IELs undergo apoptosis, lose the ability to proliferate, or migrate out of the small intestine. The adult cohort was less impacted with regard to percent reduction of IEL than the weanling and adolescent cohorts. Adults have more IELs at baseline, thus when obesity occurs, it is not as deleterious as it is for weanling and adolescent onset of obesity. Overall, the data supports the hypothesis that obesity which occurs around weaning period has further negative implications on the development of a full T cell repertoire in the intestine than the adolescent and adult onset of obesity.

The flow cytometry data does show more variable results than the immunofluorescent microscopy data. One caveat of using flow cytometry is that there are differences in cellular viability due to the rigorous IEL isolation process. Therefore, the CD3+, αβ, γδ, CD4+, and CD8α+ T cell numbers, which are based on the total number of live lymphocytes, are more variable and thus numerous experiments are required. Nevertheless, overall, previous immunofluorescent microscopy data does support and corroborate much of our flow cytometry data.

Obesity causes a reduction of CD3+, γδ, and γδ CD8α+ T cells which can have negative consequences in the intestine. Our data shows that obesity reduces γδ T cell number in the intestinal epithelium of all three cohorts of mice, and skews these T cells away from a CD8α+ phenotype in the adolescent and adult mice cohorts. However, these CD8α+ cells were unchanged in the weanling cohort. We hypothesize that the weanling mice have not yet

developed these T cell populations. When CD3+ T cells become activated, they produce cytokines and chemokines that protect against pathogens and regulate the epithelial tissue homeostasis. γδ T cells are essential because they produce growth factors to initiate epithelial proliferation and wound repair as well as cytokines that have antimicrobial properties to fight infections (Boismenu and Havran 1994, Inagaki-Ohar et al. 2004, Hamada et al. 2008, Kuhl et al. 2007, Chen et al. 2002). Studies show that reduction or depletion of γδ T cells in the intestine causes mice to have severe colitis (Park et al., submitted manuscript, Kuhl et al. 2007). γδ CD8α+ T cells protect intestinal epithelial tissue against intracellular bacteria pathogen infection and limit pathogen spreading by producing factors that increase cytolytic activity against infected intraepithelial cells (Li et al. 2011). Thus, reduced T cell numbers can increase the risk of infection and inflammation in the intestine.

HFD induced obesity skewed αβ T cells towards a CD4+ phenotype in the adolescent cohort which can have either have positive or negative consequences. Usually, αβ T cells have protective functions against viral and parasitic infections and uphold tissue integrity (Hansen et al. 2009, Muller et al. 2000, Dharakul et al.1991, Lepage et al. 1998, Kanwar et al.1986). In addition, αβ CD4+ T cells regulate bacteria in the intestine (Mehandru et al. 2004, Li et al. 2005, Epple et al. 2010). An important subset of CD4+ T cells includes Foxp3+ T regulatory T cells which play key roles in controlling inflammation (Feuere et al. 2009). In the absence of T regulatory cells, under inflammatory conditions, such as ulcerative colitis or obesity, other CD4+ T cells subsets can produce IFN-γ which further exacerbates inflammatory diseases (Simpson et al. 1997, Xiao et al. 2016). We speculate that obesity is skewing αβ T cells towards a non regulatory CD4+ phenotype so they produce inflammatory factors that cause the intestine to be

more susceptible to inflammatory disease. Further studies are warranted to verify which populations of CD4+ T cells remain in the intestine during obesity.

IELs from adolescent and adult mice fed a HFD produce increased amounts of the proinflammatory type cytokine TNF-α, but the weanling HFD mice do not. Within the IEL population, γδ, αβ, CD8α+, CD4+ T cells can produce TNF-α (Kohyama et al. 1997, Simpson et al. 1997). Studies show that this increase in TNF-α can be detrimental to wound healing and cause a higher susceptibility to inflammatory bowel disease such as colitis (Simpson et al. 1997, Taylor et al. 2010, Park et al., submitted manuscript). In the HFD fed weanling mice, we speculate that this cohort never gained the appropriate number and subsets of IELs, thus they do not exhibit changes in TNF-α cytokine production. Between 3 to 6 weeks of age the mice begin to gain IELs that produce TNF-α which upon HFD are being stimulated into action.

In the different cohorts of mice, there seems to be a trend of reduced IFN-γ production from IELs. Once γδ IELs seed into the intestine they are able to produce the effector cytokine, IFN-γ (Simpson et al. 1997). IFN-γ is important in fighting some parasitic intestinal infections (Lepage et al. 1998). Obese weanling mice may have dysfunctional IFN-γ production, however more experiments need to be performed to validate this. On the other hand, obesity in the adolescent and adult mice did not seem to alter IFN-γ production with exception of the CD4+ T cells in the adult mice. The small change in IFN-γ production may imply that these obese mice are still able to maintain some of their ability to fight infection.

Together our data reveals that the effect of feeding mice a HFD is different on the weanling cohort as compared to the adult cohort. Therefore, this may have differential implications in epithelial homeostasis and wound repair capabilities. Consequently, human children with obesity may need more interventions for weight loss to make sure they are able to

develop a normal IEL repertoire. However, translational studies are warranted to determine whether the findings in mice will be similar in humans. Extending our study further, we can attempt to restore these intestinal intraepithelial T cells that have been reduced and impaired by obesity in order to reinstate their original function to promote barrier integrity (Taylor et al. 2010, Taylor et al. 2011). Our current overall goal is to restore small intestine homeostasis, increase tissue repair efficiency, and increase life expectancy in all ages of those affected by obesity.

Figures

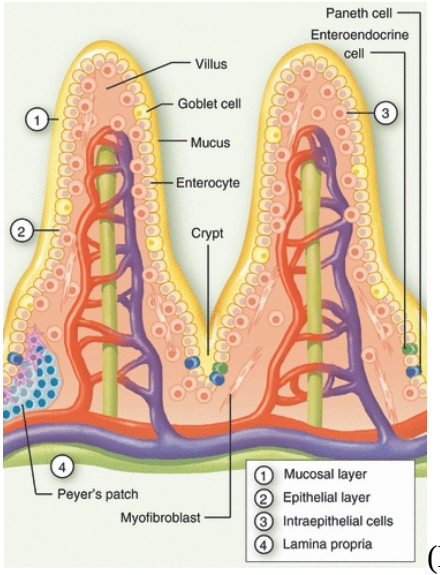

(Moenhs Veldhoen 2011)

Figure 1: Small intestine structure.

The small intestine is made up of a (1) mucosal layer and (2) epithelial layer that consist of (3) intraepithelial lymphocytes, goblet cells, Paneth cells, and enteroendocrine cells that can also be found in the (4) lamina propria. Secondary lymphoid structures, including cryptopatches and Peyer's patches are found in the lamina propria.

Table 1: Intraepithelial T cell subsets that reside in the intestine.

Natural IELs	**TCRγδ**
	CD4-/CD8-
	CD8αα
	TCRαβ
	CD4-/CD8-
	CD8αα
Induced IELs	**TCRαβ**
	CD8αβ
	CD4+
	CD4+/CD8αα

The T cell subsets in orange are types of natural intraepithelial lymphocytes (thymus differentiated) and in the blue are types of induced intraepithelial lymphocytes T cells (peripherally differentiated).

Table 2: Normal chow and high fat diet chow components.

	Normal Chow Diet (Teklad LM-485, Harlan Laboratory)	**High Fat Diet** (D12492, Research Diets)
KiloCalories from Protein (%)	25	20
KiloCalories from Fat (%)	17	60
KiloCalories from Carbohydrate (%)	58	20
Calories per 1 g of Food	3.1	5.24

(Harlan Laboratory and Research Diets)

Table 3: Mouse and human ages and staging for this study.

	Mouse Ages	Human Ages
Child	Birth-21 days	0-5 years old
Adolescent	3- 8 weeks	9-14 years old
Adult	after 10 weeks	after 19 years old

(Dutta and Sengupta 2016, Fox et al. 2007. Roscoe et al. 2007)

For this study, the different mouse stages were set as a comparison to human stages as described by Dutta and Sengupta, Fox et al., and Roscoe et al.

Table 4: Mouse cohort study timeline.

	Diet Type	Start Age	End Age
Weanling (Lean)	Normal Chow Diet	3 Weeks	10 Weeks
Weanling (Obese)	High Fat Diet	3 Weeks	10 Weeks
Adolescence (Lean)	Normal Chow Diet	6 Weeks	13 Weeks
Adolescence (Obese)	High Fat Diet	6 Weeks	13 Weeks
Early Adult (Lean)	Normal Chow Diet	10 Weeks	17 Weeks
Early Adult (Obese)	High Fat Diet	10 Weeks	17 Weeks

A timeline of diets administered for different mouse cohorts. All mice were fed a NCD from 3 weeks of age until the indicated “start age”, then the diet indicated in “diet type” was administered until the “end age”. In all three cohorts of mice were fed either NCD or HFD for 7 weeks.

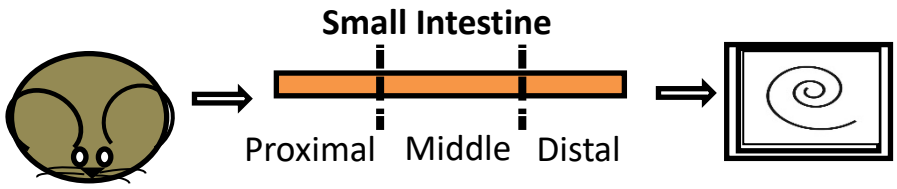

Figure 2: Small intestine embedding procedure.

The small intestine was isolated and divided into three equal parts denoted as proximal, middle, and distal. The proximal section is located nearest to the stomach and distal is the closest to the rectum. Each section were rolled with the villi side out, and frozen in OCT for histological analysis. Tissue sections were subsequently cut using a cryostat and stained with fluorescent antibodies to visualize using immunofluorescence microscopy.

A)

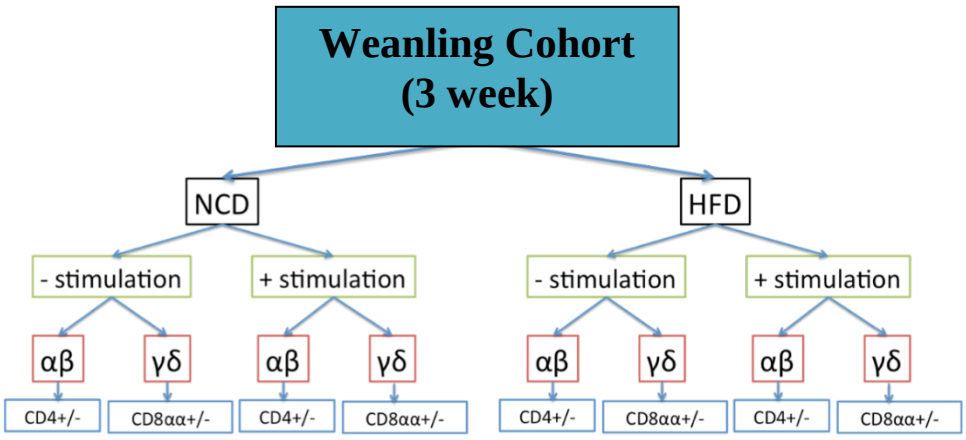

B)

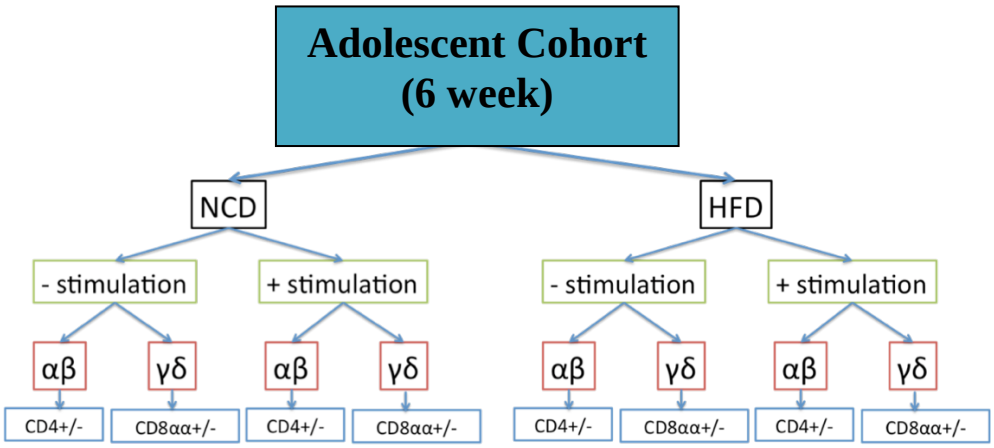

C)

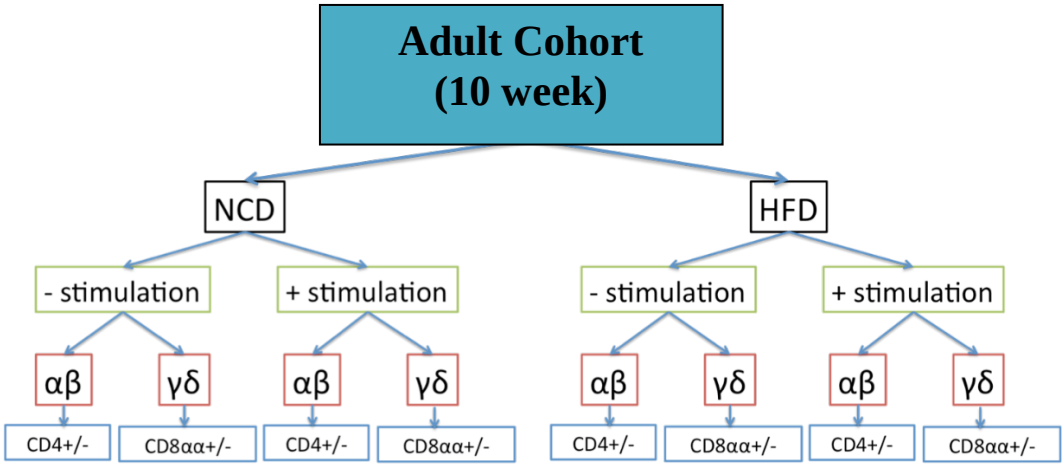

Figure 3: Flow cytometric analysis of the weanling, adolescent, adult cohorts of mice.

The mice were administered NCD or HFD at (A) 3 weeks, (B) 6 weeks, and (C) 10 weeks of age. After 7 weeks on the indicated diet, intraepithelial lymphocytes were isolated in a single cell suspension. Half of the collected cells were stimulated with the T cell mitogen Concanavalin A, while the other half received no stimulation. Cells were stained extracellularly with antibodies specific for αβ TCR, γδ TCR, and CD4, and CD8α. Subsequently, samples were also stained for intracellular cytokines TNF-α and IFN-γ and run on a flow cytometer. Data from each cohort was obtained and analyzed on the indicated populations of T cells.

Table 5: Strategy for flow cytometric analysis of isolated intraepithelial lymphocytes

Flow Cytometry Tube #	Mouse Diet	PMA	FITC	PE	PerCP/Cy5.5	APC	Label	Type of Tube
1	NCD Or HFD	-	-	-	-	-	A1	Compensation Tube
2	NCD Or HFD	-	CD3	-	-	-	A2	Compensation Tube
3	NCD Or HFD	-	-	CD3	-	-	A3	Compensation Tube
4	NCD Or HFD	-	-	-	CD3	-	A4	Compensation Tube
5	NCD Or HFD	-	-	-	-	CD3	A5	Compensation Tube
6	NCD	-	CD3	γδ TCR	CD8α	TNF-α	A10	Experimental Tube
7	NCD	+	CD3	γδ TCR	CD8α	TNF-α	A11	Experimental Tube
8	NCD	-	CD3	γδ TCR	CD8α	IFN-γ	A12	Experimental Tube
9	NCD	+	CD3	γδ TCR	CD8α	IFN-γ	B1	Experimental Tube
10	NCD	-	CD3	αβ TCR	CD4	TNF-α	B2	Experimental Tube
11	NCD	+	CD3	αβ TCR	CD4	TNF-α	B3	Experimental Tube
12	NCD	-	CD3	αβ TCR	CD4	IFN-γ	B4	Experimental Tube
13	NCD	+	CD3	αβ TCR	CD4	IFN-γ	B5	Experimental Tube
14	HFD	-	CD3	γδ TCR	CD8α	TNF-α	B6	Experimental Tube
15	HFD	+	CD3	γδ TCR	CD8α	TNF-α	B7	Experimental Tube
16	HFD	-	CD3	γδ TCR	CD8α	IFN-γ	B8	Experimental Tube
17	HFD	+	CD3	γδ TCR	CD8α	IFN-γ	B9	Experimental Tube

Flow Cytometry Tube #	Mouse Diet	PMA	FITC	PE	PerCP/Cy5.5	APC	Label	Type of Tube
18	HFD	-	CD3	αβ TCR	CD4	TNF-α	B10	Experimental Tube
19	HFD	+	CD3	αβ TCR	CD4	TNF-α	B11	Experimental Tube
20	HFD	-	CD3	αβ TCR	CD4	IFN-γ	B12	Experimental Tube
21	HFD	+	CD3	αβ TCR	CD4	IFN-γ	C1	Experimental Tube

The isolated intraepithelial lymphocytes from mice administered NCD or HFD. These intraepithelial lymphocytes were unstimulated (-) or stimulated (+) with PMA, and stained using antibodies with different fluorescent labels and analyzed using flow cytometry. Tubes 1-5 are compensation tubes which allow for standardization of fluorescence from the fluorochrome of the antibodies to standardize the flow cytometer. Tubes 6-21 were experimental tubes which were used for data analysis.

A) Normal Chow Diet High Fat Diet

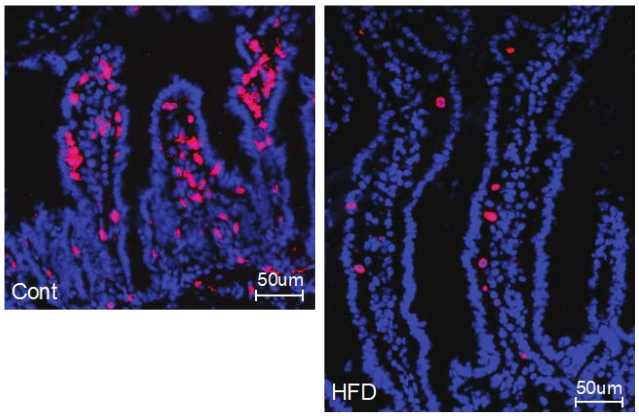

B)

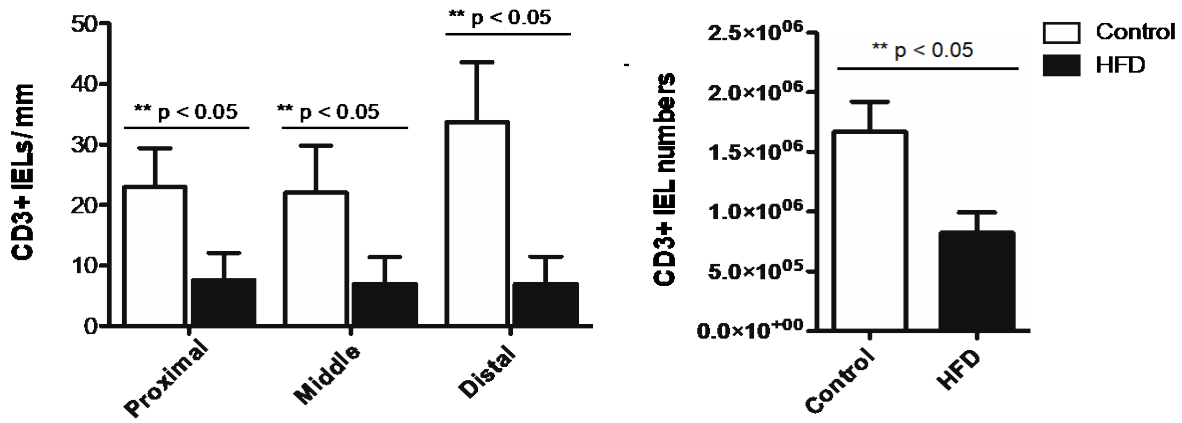

Figure 4: Obesity induces IEL loss in the proximal, middle, and distal sections of the small intestine (data submitted in manuscript, performed prior to thesis by Kitty Cheung, reproduced by Christa Park).

(A) Proximal, middle, and distal small intestine sections stained with a monoclonal antibody specific for CD3 T cells were visualized by immunofluorescence imaging. Images were captured at 20X magnification. CD3 T cells are stained in red, while the cell nuclei are stained in blue. These are representative pictures of villi from the small intestine of mice on NCD and HFD. (B) CD3 cells were counted and quantified per mm villi length. (C) Isolated intestinal epithelial cells were stained with CD3 specific antibodies and analyzed by flow cytometry. Error bars represent SD. ** represents significant P value less than <0.05. Student's unpaired *t* test was conducted using Prism Graph Pad software. Data are representative of three experiments.

A)

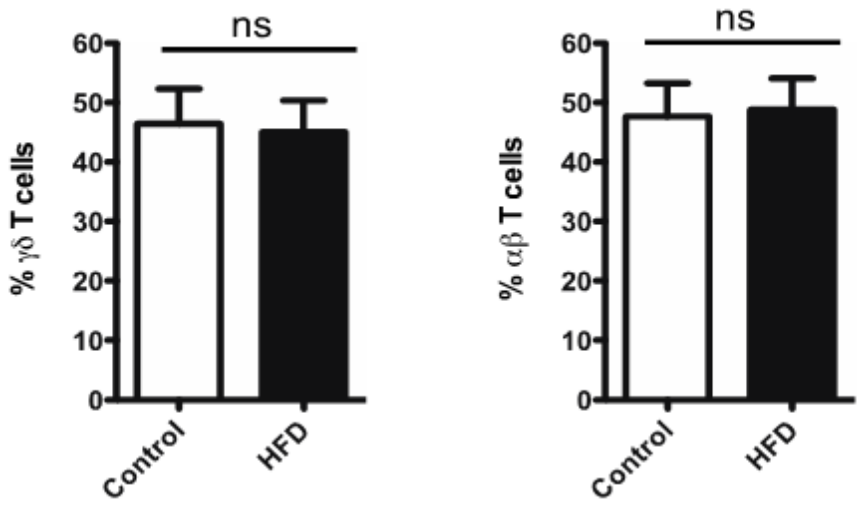

B)

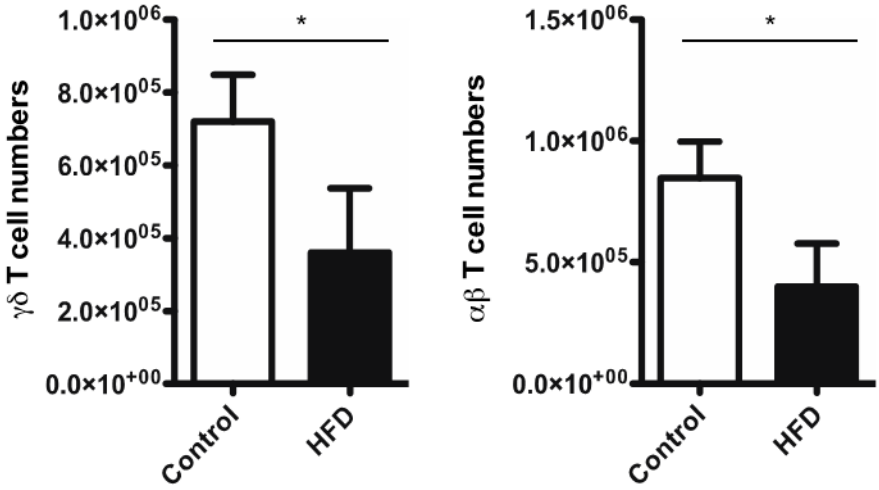

Figure 5: Obesity reduces γδ and αβ T cell subsets in the intestine (data submitted in manuscript, performed prior to thesis by Kitty Cheung, reproduced by Christa Park).

Intestinal epithelial cells were isolated and stained for γδ and αβ T cell populations and examined by flow cytometric analysis after 14 weeks on specific diet. (A) Percentages and (B) absolute cell number of αβ and γδ T cell in mice given a normal chow diet (n=3) or high fat diet (n=3). Student's unpaired *t* test was conducted using Prism Graph Pad software. * represents significant P value less than <0.05. Error bars represent SD.

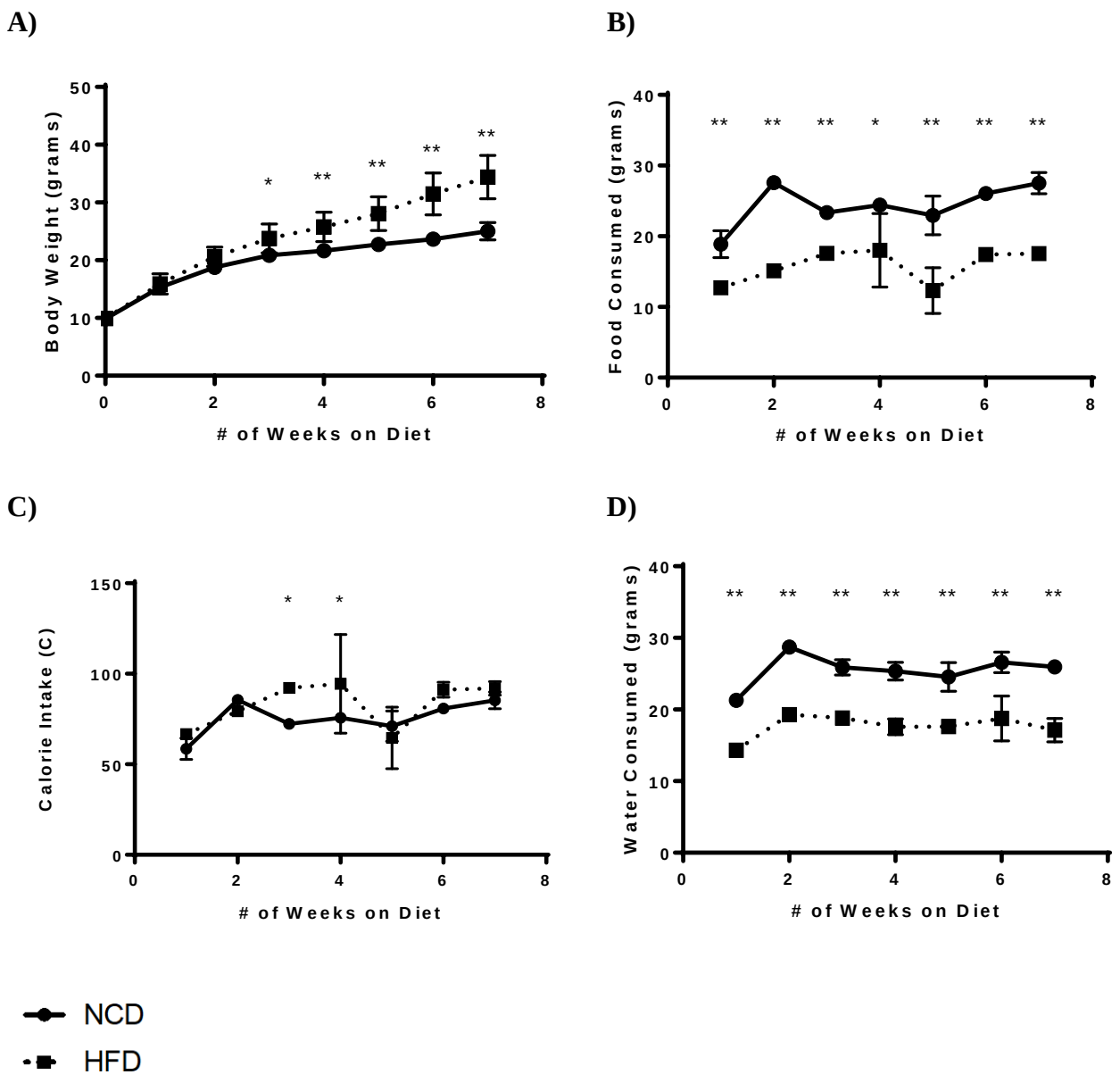

Figure 6: Weanling cohort of mice exhibit high fat diet induced obesity.

Measurements of 3 week old mice during the 7-week HFD (n=10) or NCD treatment (n=9). (A) Body weight, (B) food consumed, (C) Calorie intake, and (D) water consumed measured per week. Two-way repeated measures ANOVA was conducted using Prism Graph Pad software. * represents significant P value less than <0.05, and ** represents significant P value equal to or less than <0.0001. Error bars represent SD.

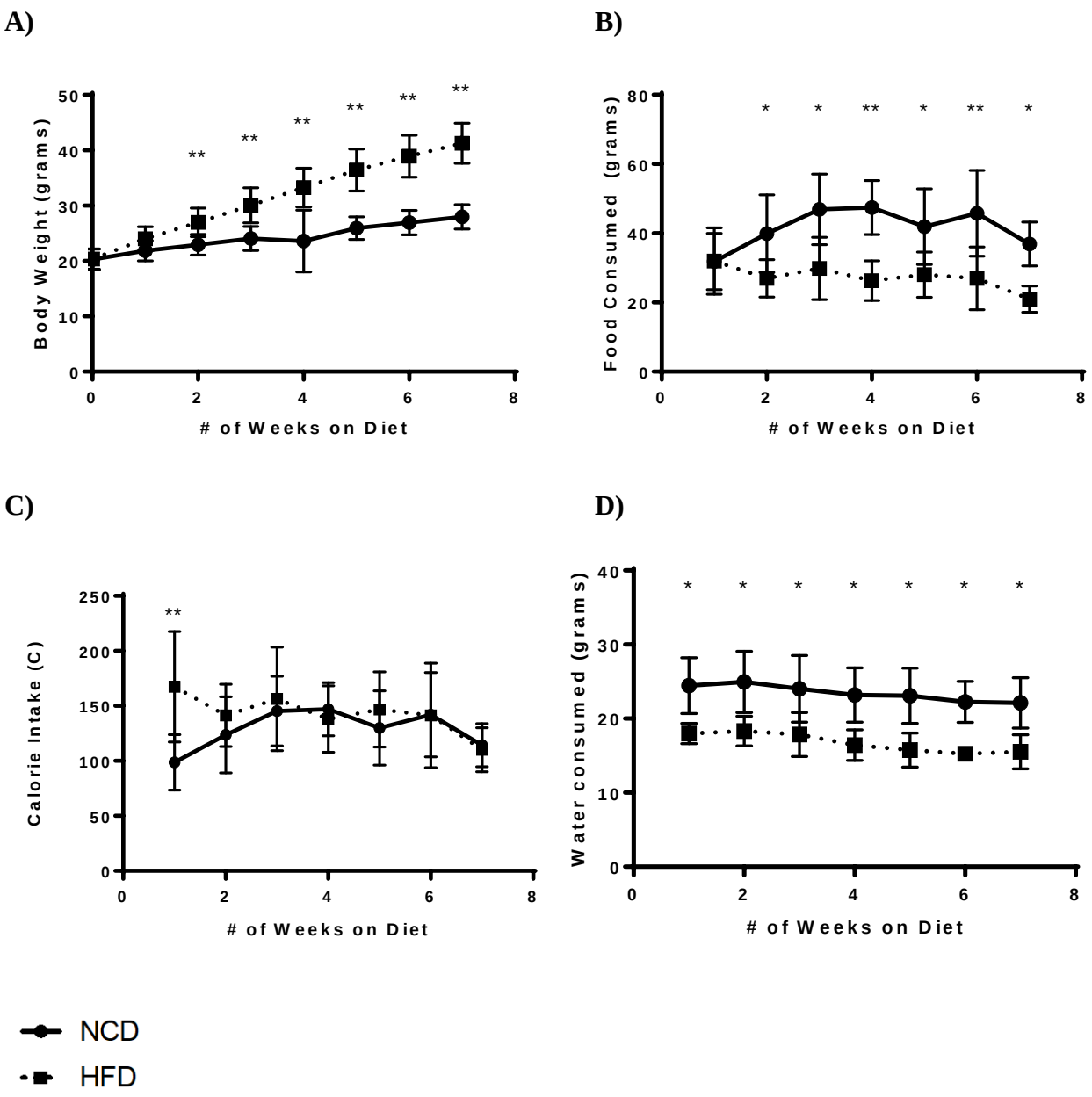

Figure 7: Adolescent cohort of mice exhibit high fat diet induced obesity.

Measurements of 6 week old mice during the 7-week HFD (n=21) or NCD treatment (n=21). (A) Body weight, (B) food consumed, (C) Calorie intake, and (D) water consumed measured per week. Two-way repeated measures ANOVA was conducted using Prism Graph Pad software. * represents significant P value less than <0.05, and ** represents significant P value equal to or less than <0.0001. Error bars represent SD.

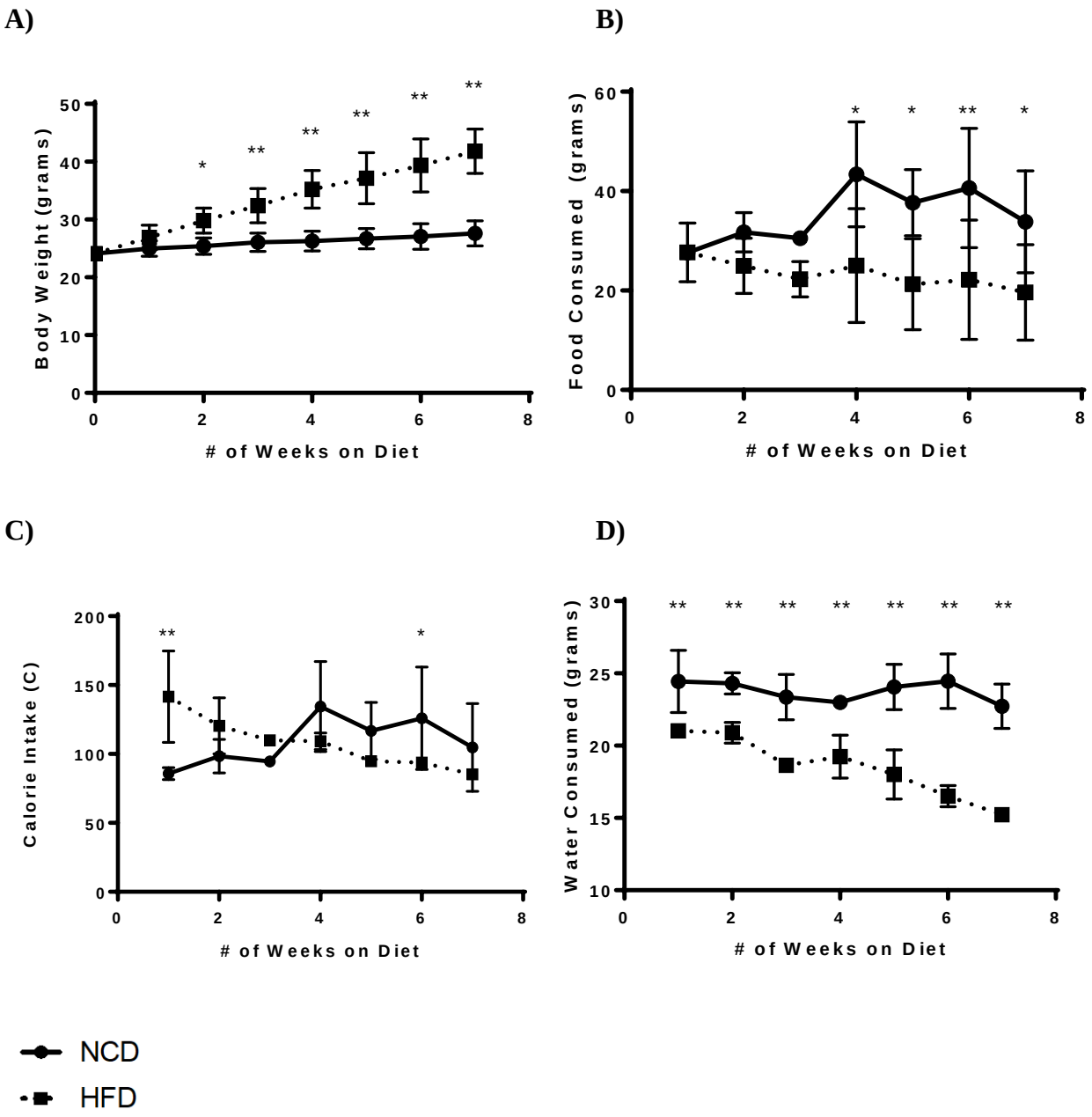

Figure 8: Adult cohort of mice exhibit high fat diet induced obesity.

Measurements of 10 week old mice during the 7-week HFD (n=12) or NCD treatment (n=12). (A) Body weight, (B) food consumed, (C) Calorie intake, and (D) water consumed measured per week. Two-way repeated measures ANOVA was conducted using Prism Graph Pad software. * represents significant P value less than <0.05, and ** represents significant P value equal to or less than <0.0001. Error bars represent SD.

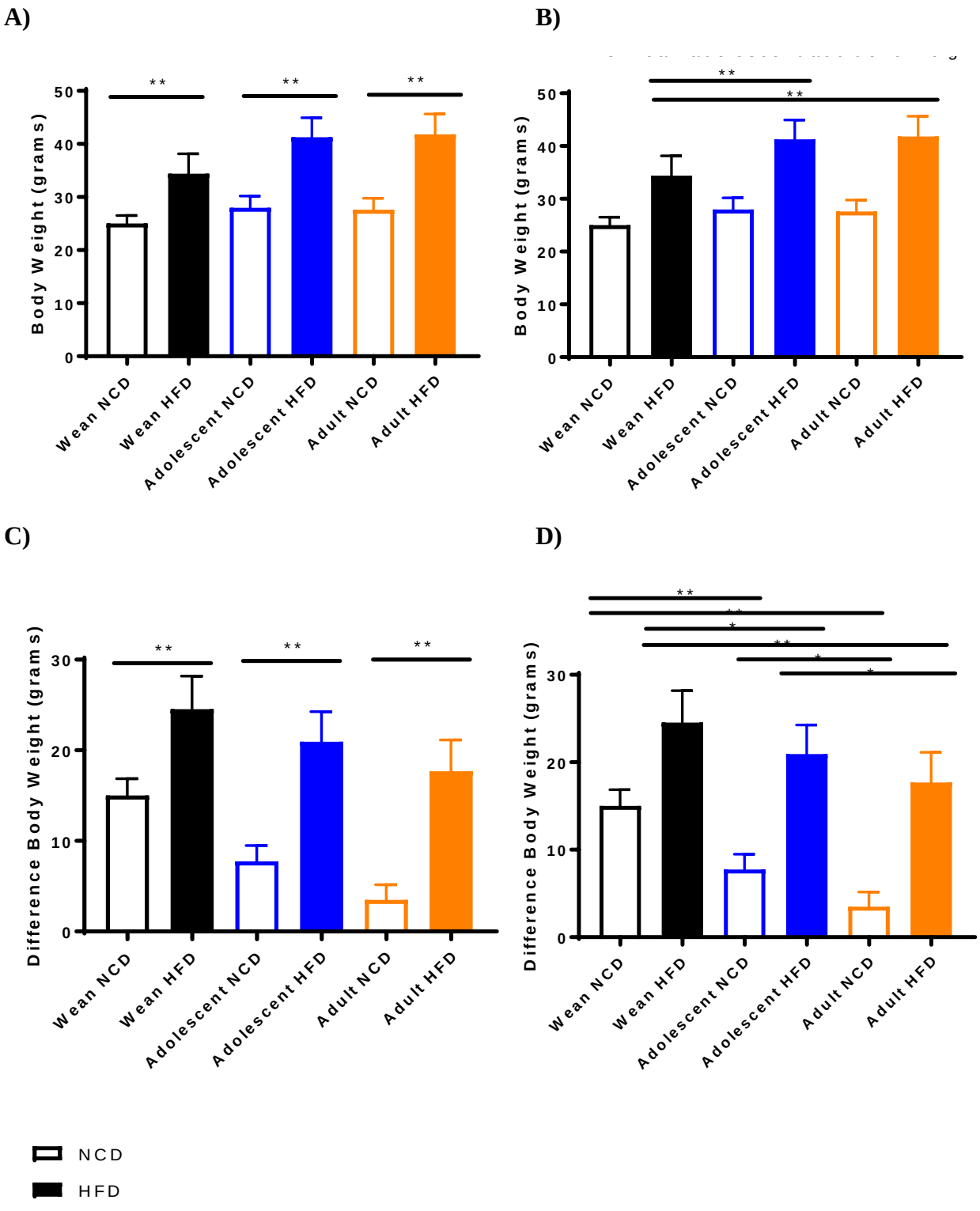

Figure 9: Weanling, adolescent, adult cohorts of mice exhibit HFD induced obesity.

Body weight of weanling (NCD n=9, HFD n=10), adolescent (NCD n=21, HFD n=21), and adult (NCD n=12, HFD n=12) mice after the 7-week HFD or NCD treatment. Average body weight at the end of the study for each of the mouse cohorts showing (A) significance within cohort (B) significance within diet treatment group. The average weight different from baseline in the different cohorts of mice (C) significance within cohort (D) significance within treatment group. Two-way repeated measures ANOVA was conducted using Prism Graph Pad software. * represents significant P value less than <0.05, and ** represents significant P value equal to or less than <0.0001. Error bars represent SD.

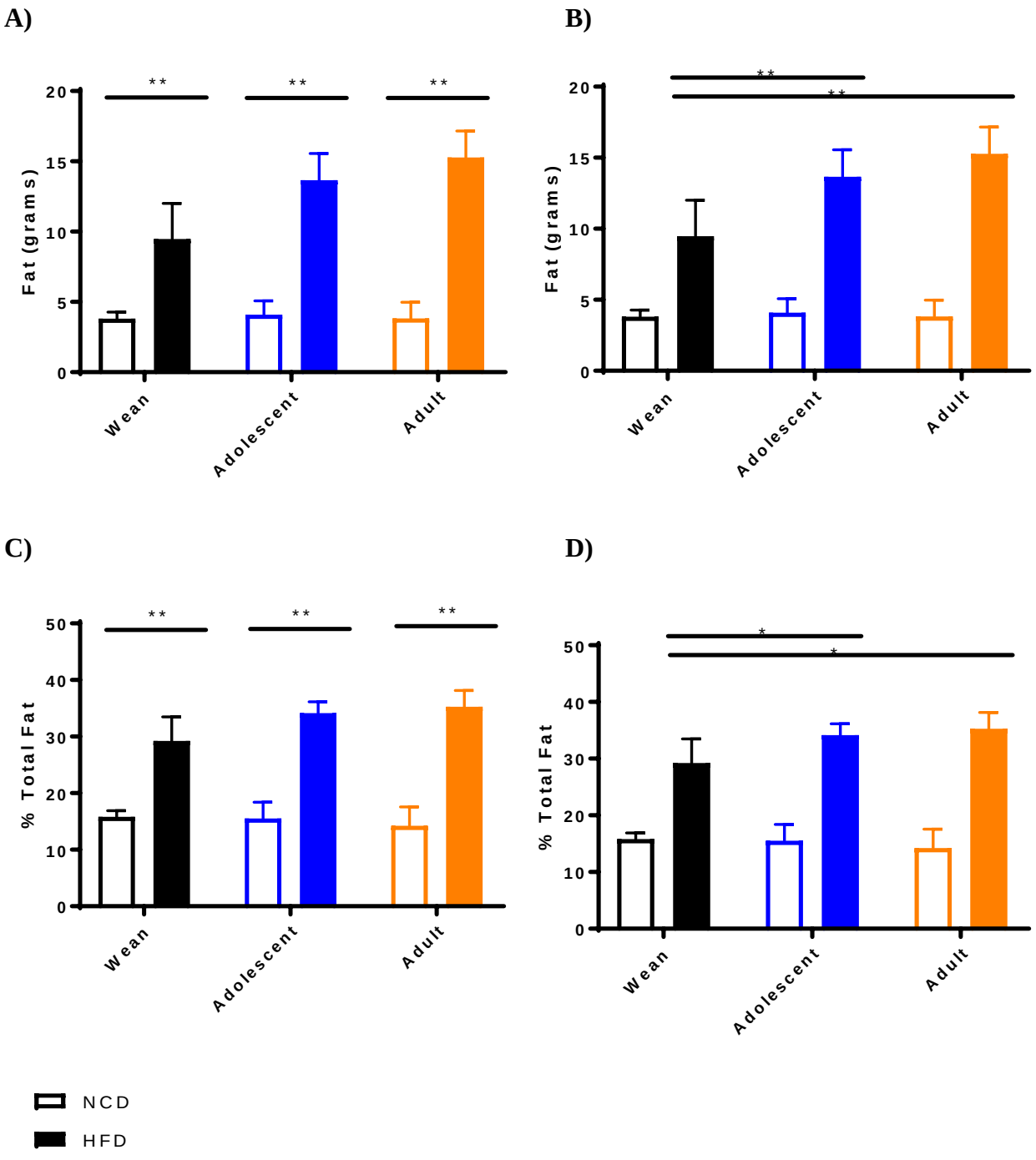

Figure 10: Weanling, adolescent, adult cohort of mice exhibit high fat diet induced obesity.

Fat mass of weanling (NCD n= 4, HFD n=6), adolescent (NCD n= 14, HFD n=13), and adult (NCD n= 8, HFD n=8) mice after the 7-week HFD or NCD treatment. The average fat mass at the end of the treatment for each of the mice cohorts showing (A) significance within cohort (B) significance within treatment group. The average percentage of fat mass from total body mass at the end of the diet treatments in each cohort of mice (C) significance within cohort (D)

significance within treatment group. Two-way repeated measures ANOVA was conducted using Prism Graph Pad software. * represents significant P value less than <0.05, and ** represents significant P value equal to or less than <0.0001. Error bars represent SD.

A)

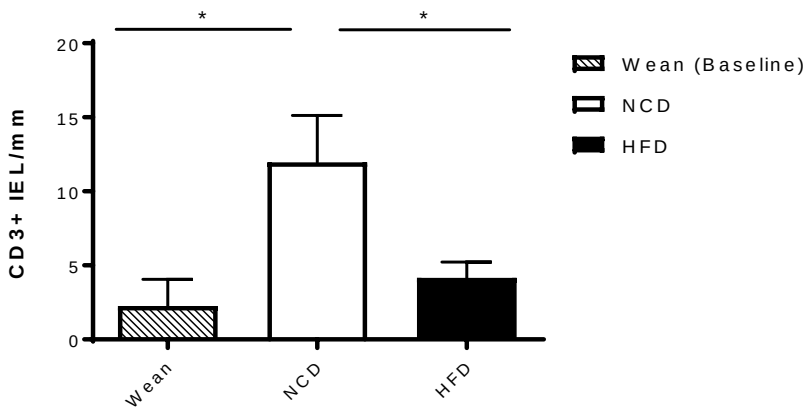

B)

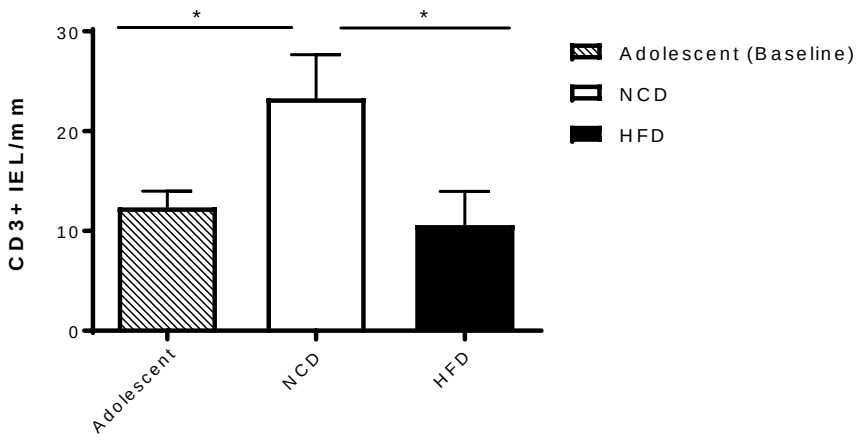

C)

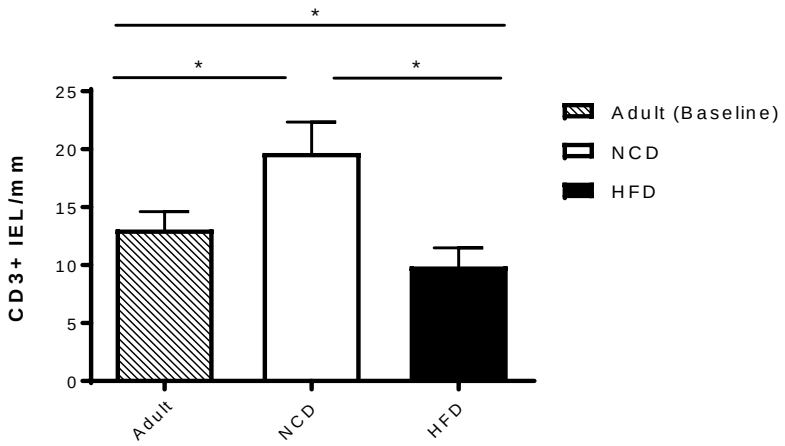

Detailed Statistical Analysis for Figure 11A

ANOVA table	DF	F (DFn, DFd)	P value
Treatment (between columns)	2	F (2, 13) = 28.12	P<0.0001
Residual (within columns)	13		
Total	15		

Tukey's multiple comparisons test	Adjusted P Value
Wean vs. NCD	<0.0001
Wean vs. HFD	0.4145
NCD vs. HFD	0.0001

Detailed Statistical Analysis for Figure 11B

ANOVA table	DF	F (DFn, DFd)	P value
Treatment (between columns)	2	F (2, 13) = 22.26	P<0.0001
Residual (within columns)	13		
Total	15		

Tukey's multiple comparisons test	Adjusted P Value
Adolescent vs. NCD	0.0009
Adolescent vs. HFD	0.7173
NCD vs. HFD	<0.0001

Detailed Statistical Analysis for Figure 11C

ANOVA table	DF	F (DFn, DFd)	P value
Treatment (between columns)	2	F (2, 11) = 27.51	P<0.0001
Residual (within columns)	11		
Total	13		

Tukey's multiple comparisons test	Adjusted P Value
Adult vs. NCD	0.0015
Adult vs. HFD	0.1316

Tukey's multiple comparisons test	Adjusted P Value
NCD vs. HFD	<0.0001

Figure 11: Weanling, adolescent, and adult cohorts of mice administered HFD exhibit reduced numbers of CD3+ IEL.

Weanling, adolescent, and adult cohorts of mice administered a HFD exhibited reduced numbers of CD3+ IEL per mm villi length. CD3+ IELs per mm villi length of the proximal portion of the small intestine of (A) weanling (baseline n=4, NCD n=6, HFD n=6), (B) adolescent (baseline n=4, NCD n=6, HFD n=6), and (C) adult (baseline n=4, NCD n=6, and HFD n=4) mice fed a HFD or NCD. One-way ANOVA was conducted using Prism Graph Pad software.* represents significant P value less than <0.05. Error bars represent SD.

A) Weanling Baseline **Weanling NCD** **Weanling HFD**

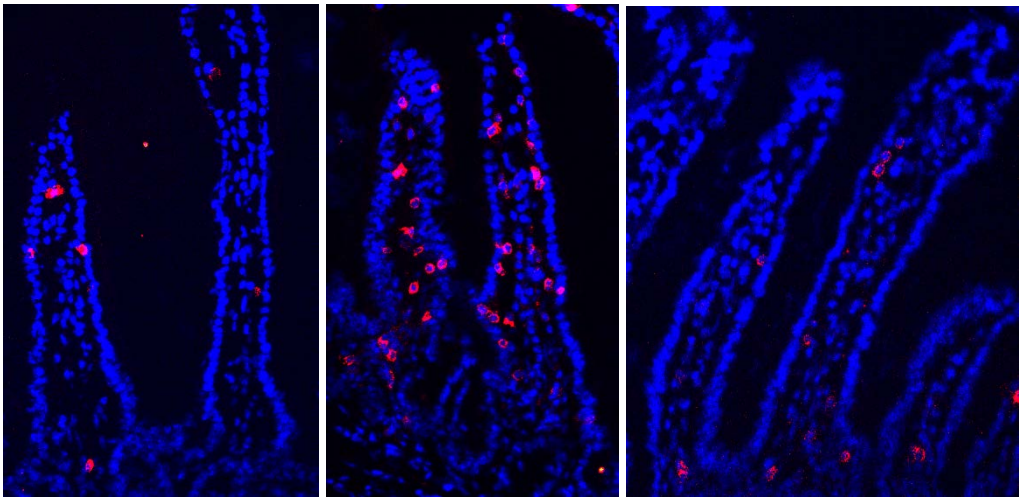

B) Adolescent Baseline **Adolescent NCD** **Adolescent HFD**

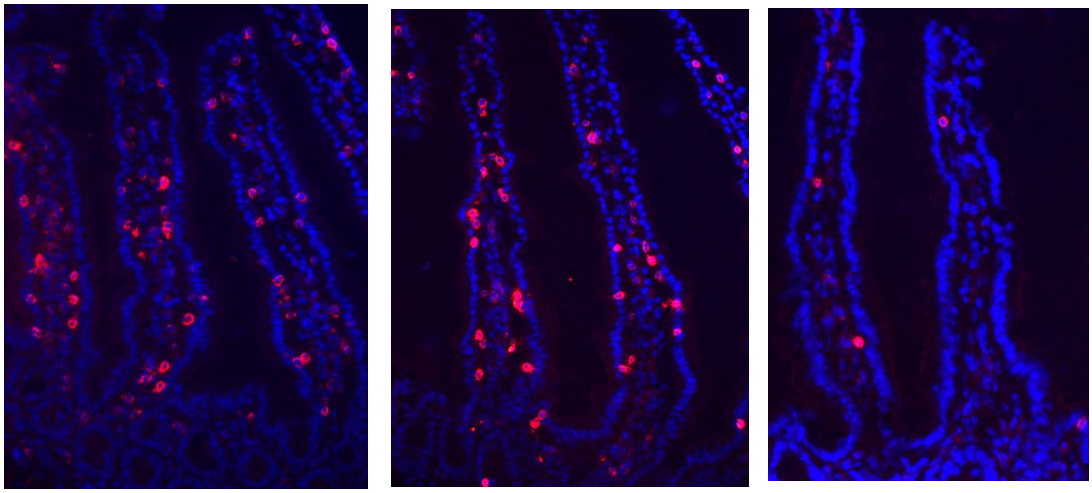

C) Adult Baseline **Adult NCD** **Adult HFD**

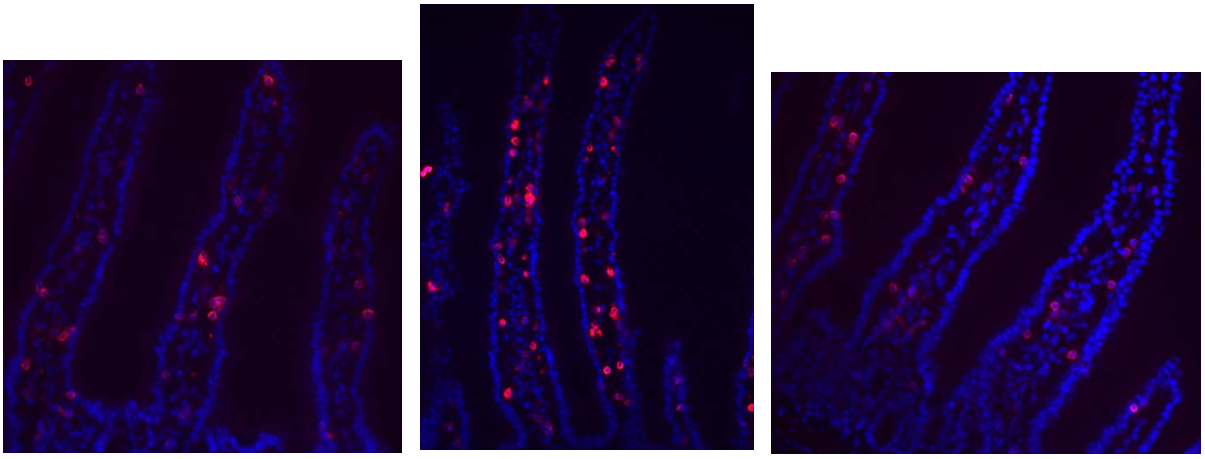

CD3+ Cells

Cell Nuclei (DAPI)

Figure 12: Weanling, adolescent, adult cohorts of mice treated with HFD have reduced CD3+ IEL.

These are representative immunofluorescent images of villi from the small intestine of (A) weanling (B) adolescent (C) adult cohorts of mice at baseline and after NCD or HFD treatment. CD3 T cells are stained in red, while the cell nuclei are stained in blue. Villi images were captured at 20X magnification. Data are representative of three experiments.

Table 6: Weanling, adolescent, adult cohorts of mice treated with HFD have reduced CD3+ IEL.

Mouse Cohorts	AVG IEL #/mm	% Change between NCD and HFD	Normalized to baseline fold change)	N Sample Size
Weanling (Baseline)	3	-	1.0	4
Weanling NCD	12	-	4.5	6
Weanling HFD	4	-	1.6	6
Change between weanling NCD and HFD	8	65	-	-
Adolescent (Baseline)	12	-	1.0	4
Adolescent NCD	23	-	1.9	6
Adolescent HFD	11	-	0.9	6
Change between adolescent NCD and HFD	13	55	-	-
Adult (Baseline)	13	-	1.0	4
Adult NCD	20	-	1.5	6
Adult HFD	10	-	0.8	4
Change between adult NCD and HFD	10	50	-	-

Weanling, adolescent, and adult cohorts of mice treated with HFD for 7 weeks exhibited reduced CD3+ IEL per mm villi length. The average IEL number per mm from Figure 12 and the percent IEL change comparing the NCD number per mm to the HFD IEL number per mm in the different mice cohorts. In addition, baseline was normalized in each cohort of mice to determine the fold change of the NCD and HFD IEL number per mm.

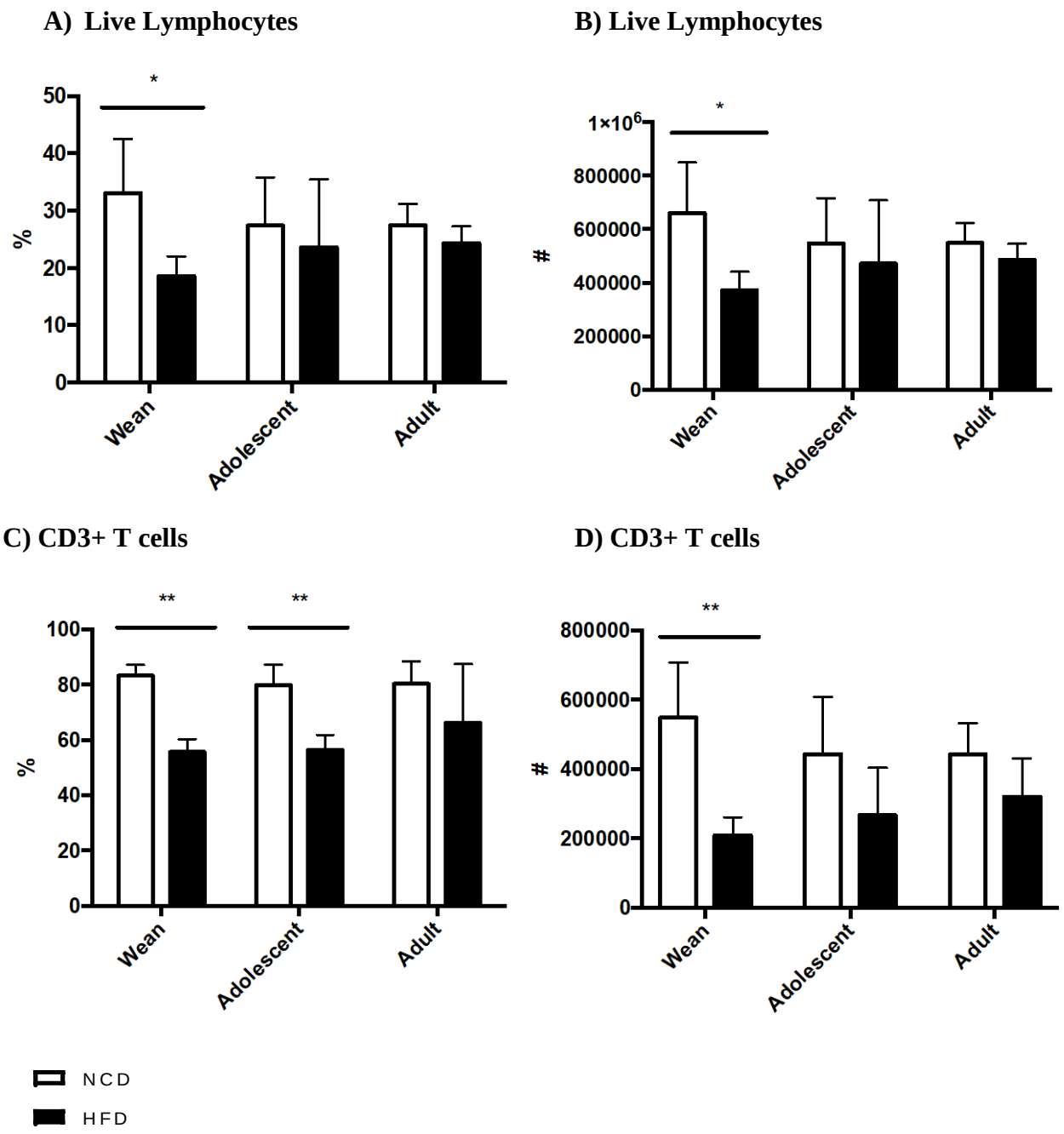

Detailed Statistical Analysis for Figure 13A

ANOVA table	DF	F (DFn, DFd)	P value
Interaction	2	F (2, 27) = 1.695	P=0.2026
Row Factor	2	F (2, 27) = 0.007926	P=0.9921
Column Factor	1	F (1, 27) = 7.003	P=0.0134
Residual	27		

Tukey's multiple comparisons test	Adjusted P Value
Wean:NCD vs. Wean:HFD	0.0844
Wean:NCD vs. Adolescent:NCD	0.7827
Wean:NCD vs. Adolescent:HFD	0.4587
Wean:NCD vs. Adult:NCD	0.799
Wean:NCD vs. Adult:HFD	0.5415
Wean:HFD vs. Adolescent:NCD	0.3578
Wean:HFD vs. Adolescent:HFD	0.92
Wean:HFD vs. Adult:NCD	0.3743
Wean:HFD vs. Adult:HFD	0.8698
Adolescent:NCD vs. Adolescent:HFD	0.9515
Adolescent:NCD vs. Adult:NCD	>0.9999
Adolescent:NCD vs. Adult:HFD	0.9798
Adolescent:HFD vs. Adult:NCD	0.9537
Adolescent:HFD vs. Adult:HFD	>0.9999
Adult:NCD vs. Adult:HFD	0.9806

Detailed Statistical Analysis for Figure 13B

ANOVA table	DF	F (DFn, DFd)	P value
Interaction	2	F (2, 27) = 1.695	P=0.2026
Row Factor	2	F (2, 27) = 0.007926	P=0.9921
Column Factor	1	F (1, 27) = 7.003	P=0.0134
Residual	27		

Tukey's multiple comparisons test	Adjusted P Value
Wean:NCD vs. Wean:HFD	0.0844
Wean:NCD vs. Adolescent:NCD	0.7827
Wean:NCD vs. Adolescent:HFD	0.4587
Wean:NCD vs. Adult:NCD	0.799
Wean:NCD vs. Adult:HFD	0.5415
Wean:HFD vs. Adolescent:NCD	0.3578
Wean:HFD vs. Adolescent:HFD	0.92
Wean:HFD vs. Adult:NCD	0.3743

Tukey's multiple comparisons test	Adjusted P Value
Wean:HFD vs. Adult:HFD	0.8698
Adolescent:NCD vs. Adolescent:HFD	0.9515
Adolescent:NCD vs. Adult:NCD	>0.9999
Adolescent:NCD vs. Adult:HFD	0.9798
Adolescent:HFD vs. Adult:NCD	0.9537
Adolescent:HFD vs. Adult:HFD	>0.9999
Adult:NCD vs. Adult:HFD	0.9806

Detailed Statistical Analysis for Figure 13C

ANOVA table	DF	F (DFn, DFd)	P value
Interaction	2	F (2, 27) = 1.278	P=0.2950
Row Factor	2	F (2, 27) = 0.8272	P=0.4481
Column Factor	1	F (1, 27) = 37.78	P<0.0001
Residual	27		

Tukey's multiple comparisons test	Adjusted P Value
Wean:NCD vs. Wean:HFD	0.0041
Wean:NCD vs. Adolescent:NCD	0.991
Wean:NCD vs. Adolescent:HFD	0.0057
Wean:NCD vs. Adult:NCD	0.9956
Wean:NCD vs. Adult:HFD	0.1524
Wean:HFD vs. Adolescent:NCD	0.0029
Wean:HFD vs. Adolescent:HFD	>0.9999
Wean:HFD vs. Adult:NCD	0.0029
Wean:HFD vs. Adult:HFD	0.6179
Adolescent:NCD vs. Adolescent:HFD	0.0043
Adolescent:NCD vs. Adult:NCD	>0.9999
Adolescent:NCD vs. Adult:HFD	0.1979
Adolescent:HFD vs. Adult:NCD	0.0043
Adolescent:HFD vs. Adult:HFD	0.6989
Adult:NCD vs. Adult:HFD	0.1877

Detailed Statistical Analysis for Figure 13D

ANOVA table	DF	F (DFn, DFd)	P value
Interaction	2	F (2, 27) = 1.71	P=0.1998
Row Factor	2	F (2, 27) = 0.1378	P=0.8719
Column Factor	1	F (1, 27) = 19.78	P=0.0001
Residual	27		

Tukey's multiple comparisons test	Adjusted P Value
Wean:NCD vs. Wean:HFD	0.0106
Wean:NCD vs. Adolescent:NCD	0.7474
Wean:NCD vs. Adolescent:HFD	0.0466
Wean:NCD vs. Adult:NCD	0.7557
Wean:NCD vs. Adult:HFD	0.1592
Wean:HFD vs. Adolescent:NCD	0.0553
Wean:HFD vs. Adolescent:HFD	0.9878
Wean:HFD vs. Adult:NCD	0.064
Wean:HFD vs. Adult:HFD	0.8221
Adolescent:NCD vs. Adolescent:HFD	0.2373
Adolescent:NCD vs. Adult:NCD	>0.9999
Adolescent:NCD vs. Adult:HFD	0.6184
Adolescent:HFD vs. Adult:NCD	0.2596
Adolescent:HFD vs. Adult:HFD	0.9906
Adult:NCD vs. Adult:HFD	0.6433

Figure 13: Weanling, adolescent, adult cohorts of mice treated with HFD have reduced CD3+ IEL.

Epithelial cells isolated from the small intestine of weanling (NCD n= 4, HFD n=4), adolescent (NCD n= 8, HFD n=4), and adult (NCD n= 8, HFD n=4) cohort of mice after 7 week HFD or NCD treatment. Cells were stained for CD3 expression and analyzed by flow cytometry. (A) Percentages and absolute cell counts of live cells and (B) CD3+ T cells percentages and absolute cell counts based on total number of live lymphocytes. Two-way ANOVA was conducted using Prism Graph Pad software. * represents significant P value less than <0.05, and ** represents significant P value equal to or less than <0.01. Error bars represent SD.

A) γδ T Cells

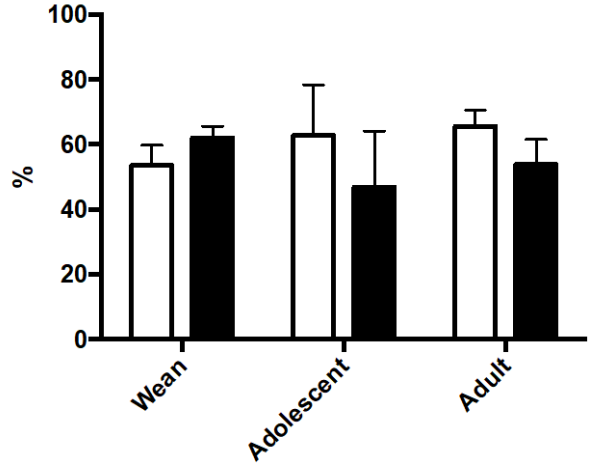

B) γδ T Cells

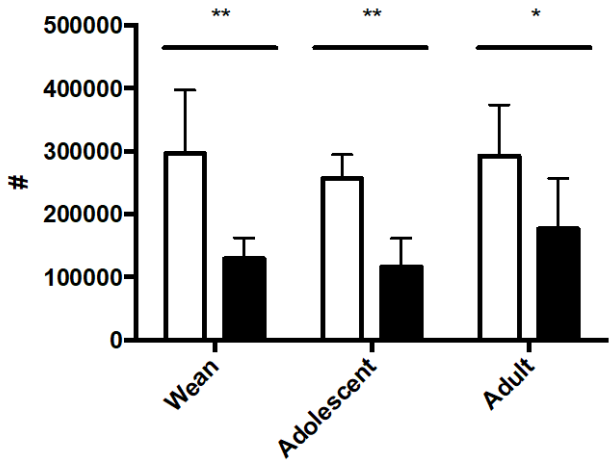

C) γδ CD8α+ T cells

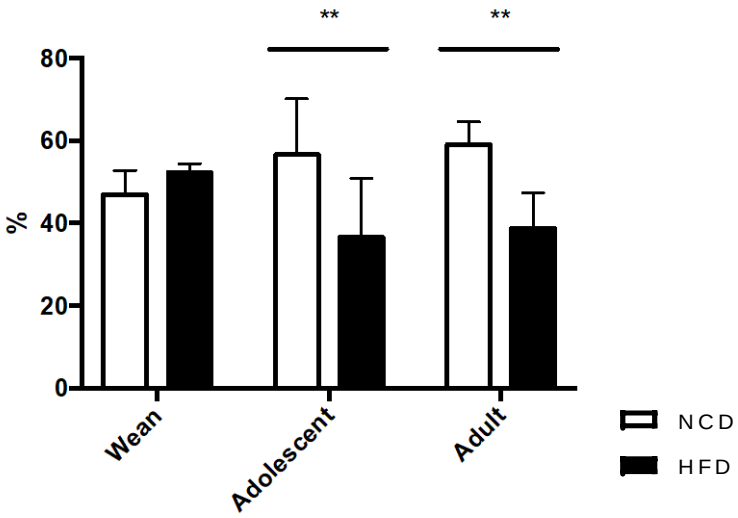

Detailed Statistical Analysis for Figure 14A

ANOVA table	DF	F (DFn, DFd)	P value
Interaction	2	F (2, 27) = 3.091	P=0.0618
Row Factor	2	F (2, 27) = 0.5417	P=0.5879
Column Factor	1	F (1, 27) = 2.394	P=0.1335
Residual	27		

Tukey's multiple comparisons test	Adjusted P Value
Wean:NCD vs. Wean:HFD	0.8802
Wean:NCD vs. Adolescent:NCD	0.7301
Wean:NCD vs. Adolescent:HFD	0.9548
Wean:NCD vs. Adult:NCD	0.4965
Wean:NCD vs. Adult:HFD	>0.9999
Wean:HFD vs. Adolescent:NCD	>0.9999
Wean:HFD vs. Adolescent:HFD	0.3993
Wean:HFD vs. Adult:NCD	0.9951
Wean:HFD vs. Adult:HFD	0.899
Adolescent:NCD vs. Adolescent:HFD	0.1934
Adolescent:NCD vs. Adult:NCD	0.9951
Adolescent:NCD vs. Adult:HFD	0.7629
Adolescent:HFD vs. Adult:NCD	0.0959
Adolescent:HFD vs. Adult:HFD	0.9431
Adult:NCD vs. Adult:HFD	0.5314

Detailed Statistical Analysis for Figure 14B

ANOVA table	DF	F (DFn, DFd)	P value
Interaction	2	F (2, 27) = 0.3425	P=0.7130
Row Factor	2	F (2, 27) = 1.469	P=0.2481
Column Factor	1	F (1, 27) = 33.84	P<0.0001
Residual	27		

Tukey's multiple comparisons test	Adjusted P Value
Wean:NCD vs. Wean:HFD	0.0142
Wean:NCD vs. Adolescent:NCD	0.9151
Wean:NCD vs. Adolescent:HFD	0.0072
Wean:NCD vs. Adult:NCD	>0.9999
Wean:NCD vs. Adult:HFD	0.137
Wean:HFD vs. Adolescent:NCD	0.0333
Wean:HFD vs. Adolescent:HFD	0.9998
Wean:HFD vs. Adult:NCD	0.0044
Wean:HFD vs. Adult:HFD	0.9061

Tukey's multiple comparisons test	Adjusted P Value
Adolescent:NCD vs. Adolescent:HFD	0.0155
Adolescent:NCD vs. Adult:NCD	0.8644
Adolescent:NCD vs. Adult:HFD	0.3475
Adolescent:HFD vs. Adult:NCD	0.0019
Adolescent:HFD vs. Adult:HFD	0.7825
Adult:NCD vs. Adult:HFD	0.0716

Detailed Statistical Analysis for Figure 14C

ANOVA table	DF	F (DFn, DFd)	P value
Interaction	2	F (2, 27) = 4.908	P=0.0152
Row Factor	2	F (2, 27) = 0.2621	P=0.7714
Column Factor	1	F (1, 27) = 10.17	P=0.0036
Residual	27		

Tukey's multiple comparisons test	Adjusted P Value
Wean:NCD vs. Wean:HFD	0.97
Wean:NCD vs. Adolescent:NCD	0.5889
Wean:NCD vs. Adolescent:HFD	0.6733
Wean:NCD vs. Adult:NCD	0.366
Wean:NCD vs. Adult:HFD	0.8435
Wean:HFD vs. Adolescent:NCD	0.978
Wean:HFD vs. Adolescent:HFD	0.2441
Wean:HFD vs. Adult:NCD	0.8717
Wean:HFD vs. Adult:HFD	0.3959
Adolescent:NCD vs. Adolescent:HFD	0.0243
Adolescent:NCD vs. Adult:NCD	0.9952
Adolescent:NCD vs. Adult:HFD	0.056
Adolescent:HFD vs. Adult:NCD	0.0106
Adolescent:HFD vs. Adult:HFD	0.9996
Adult:NCD vs. Adult:HFD	0.0252

Figure 14: Obesity reduces γδ T cell number in the intestinal epithelium of all three cohorts of mice, and skews these T cells away from a CD8α phenotype in adolescent and adult mice.

Epithelial cells isolated from the small intestine of weanling (NCD n= 4, HFD n=4), adolescent (NCD n= 8, HFD n=4), and adult (NCD n= 8, HFD n=4) cohort of mice after 7 week HFD or NCD treatment. Epithelial cells were stained for CD3, γδ, CD8α T cells and analyzed by flow cytometry. (A) Percentages and absolute cell counts of γδ T cells gated from CD3 T cell which were gated on live lymphocyte population. (B) Percentage of γδ T cells expressing CD8α. Two-way ANOVA was conducted using Prism Graph Pad software). * represents significant P value less than <0.05, and ** represents significant P value equal to or less than <0.01. Error bars represent SD.

A) αβ T cells

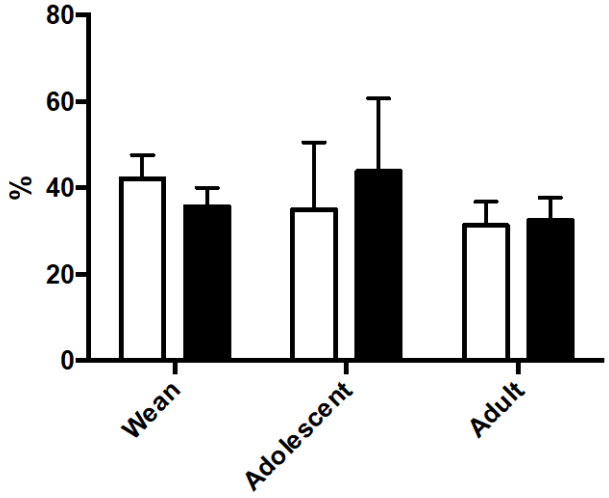

B) αβ T cells

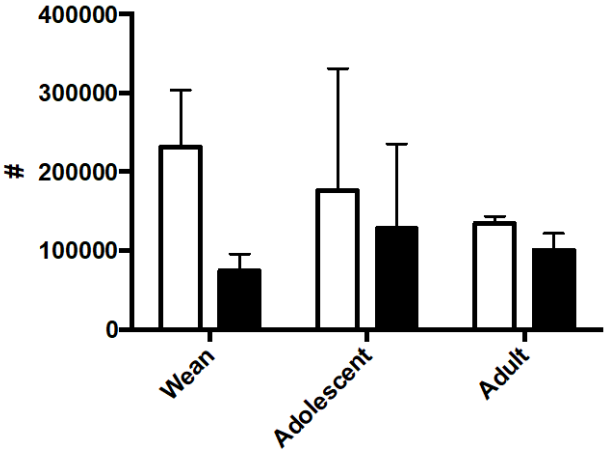

C) αβ CD4+ T cells

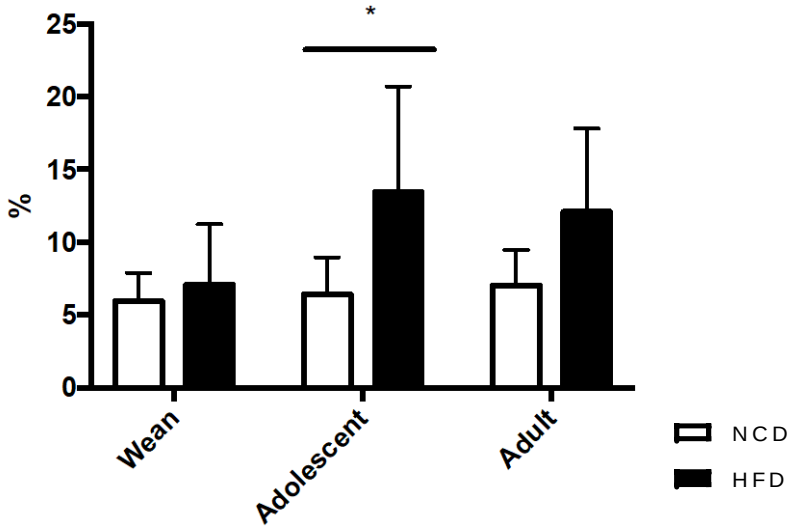

Detailed Statistical Analysis for Figure 15A

ANOVA table	DF	F (DFn, DFd)	P value
Interaction	2	F (2, 27) = 1.137	P=0.3356
Row Factor	2	F (2, 27) = 1.529	P=0.2349
Column Factor	1	F (1, 27) = 0.07939	P=0.7803
Residual	27		

Tukey's multiple comparisons test	Adjusted P Value
Wean:NCD vs. Wean:HFD	0.9566
Wean:NCD vs. Adolescent:NCD	0.882
Wean:NCD vs. Adolescent:HFD	>0.9999
Wean:NCD vs. Adult:NCD	0.5894
Wean:NCD vs. Adult:HFD	0.8077
Wean:HFD vs. Adolescent:NCD	>0.9999
Wean:HFD vs. Adolescent:HFD	0.8976
Wean:HFD vs. Adult:NCD	0.9855
Wean:HFD vs. Adult:HFD	0.9984
Adolescent:NCD vs. Adolescent:HFD	0.7672
Adolescent:NCD vs. Adult:NCD	0.9799
Adolescent:NCD vs. Adult:HFD	0.9988
Adolescent:HFD vs. Adult:NCD	0.4456
Adolescent:HFD vs. Adult:HFD	0.6937
Adult:NCD vs. Adult:HFD	>0.9999

Detailed Statistical Analysis for Figure 15B

ANOVA table	DF	F (DFn, DFd)	P value
Interaction	2	F (2, 27) = 1.084	P=0.3526
Row Factor	2	F (2, 27) = 0.4609	P=0.6356
Column Factor	1	F (1, 27) = 5.078	P=0.0326
Residual	27		

Tukey's multiple comparisons test	Adjusted P Value
Wean:NCD vs. Wean:HFD	0.22
Wean:NCD vs. Adolescent:NCD	0.9266
Wean:NCD vs. Adolescent:HFD	0.6487
Wean:NCD vs. Adult:NCD	0.5709
Wean:NCD vs. Adult:HFD	0.4009
Wean:HFD vs. Adolescent:NCD	0.4987
Wean:HFD vs. Adolescent:HFD	0.9665
Wean:HFD vs. Adult:NCD	0.905
Wean:HFD vs. Adult:HFD	0.9988

Tukey's multiple comparisons test	Adjusted P Value
Adolescent:NCD vs. Adolescent:HFD	0.957
Adolescent:NCD vs. Adult:NCD	0.9433
Adolescent:NCD vs. Adult:HFD	0.7699
Adolescent:HFD vs. Adult:NCD	>0.9999
Adolescent:HFD vs. Adult:HFD	0.9983
Adult:NCD vs. Adult:HFD	0.9912

Detailed Statistical Analysis for Figure 15C

ANOVA table	DF	F (DFn, DFd)	P value
Interaction	2	F (2, 27) = 1.339	P=0.2789
Row Factor	2	F (2, 27) = 2.021	P=0.1520
Column Factor	1	F (1, 27) = 9.141	P=0.0054
Residual	27		

Tukey's multiple comparisons test	Adjusted P Value
Wean:NCD vs. Wean:HFD	0.9986
Wean:NCD vs. Adolescent:NCD	>0.9999
Wean:NCD vs. Adolescent:HFD	0.1076
Wean:NCD vs. Adult:NCD	0.9975
Wean:NCD vs. Adult:HFD	0.2669
Wean:HFD vs. Adolescent:NCD	0.9998
Wean:HFD vs. Adolescent:HFD	0.2272
Wean:HFD vs. Adult:NCD	>0.9999
Wean:HFD vs. Adult:HFD	0.4766
Adolescent:NCD vs. Adolescent:HFD	0.0597
Adolescent:NCD vs. Adult:NCD	0.9995
Adolescent:NCD vs. Adult:HFD	0.1913
Adolescent:HFD vs. Adult:NCD	0.1142
Adolescent:HFD vs. Adult:HFD	0.996
Adult:NCD vs. Adult:HFD	0.3161

Figure 15: Obesity does not change αβ T cells percentages or numbers but skews these αβ T cells toward a CD4+ phenotype in the adolescent mouse cohort.

Epithelial cells isolated from the small intestine of weanling (NCD n= 4, HFD n=4), adolescent (NCD n= 8, HFD n=4), and adult (NCD n= 8, HFD n=4) cohort of mice after 7 week HFD or NCD treatment. Epithelial cells were stained for CD3, αβ, CD4+ T cells and analyzed by flow cytometry. (A) Percentages and absolute cell counts of αβ T cells gated from live CD3+ T cells. (B) Percentage of αβ T cells expressing CD4. Two-way ANOVA was conducted using Prism Graph Pad software. * represents significant P value less than <0.05, and ** represents significant P value equal to or less than <0.01. Error bars represent SD.

A) CD3 T cells producing TNF-α

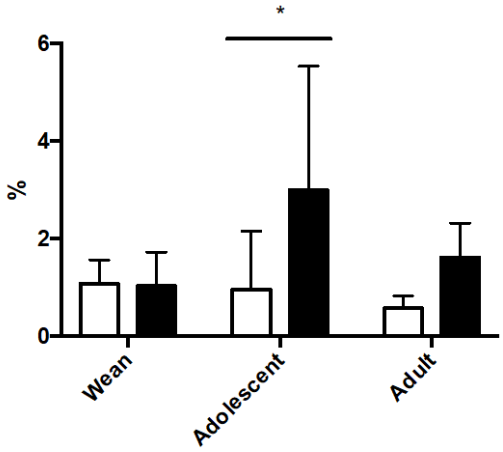

B) γδ T cells producing TNF-α

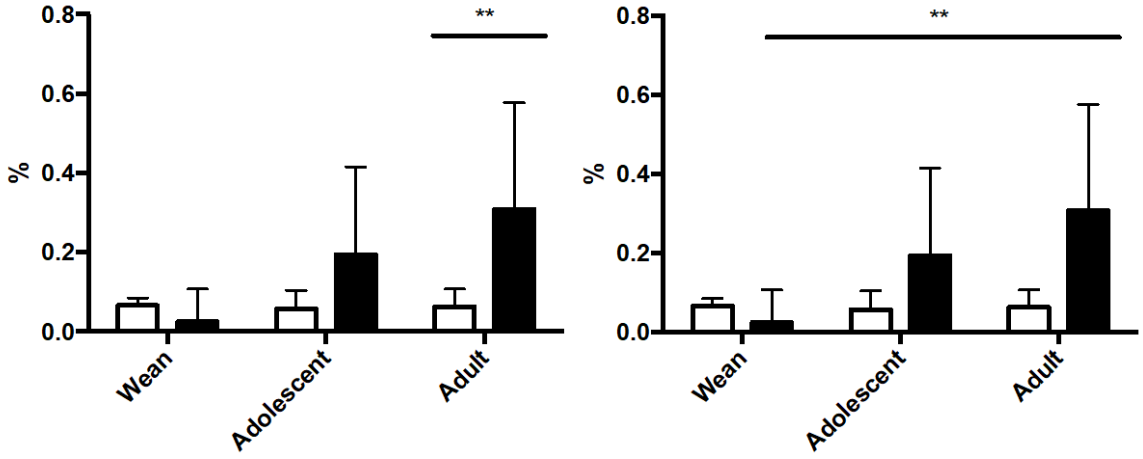

C) CD8α T cells producing TNF-α

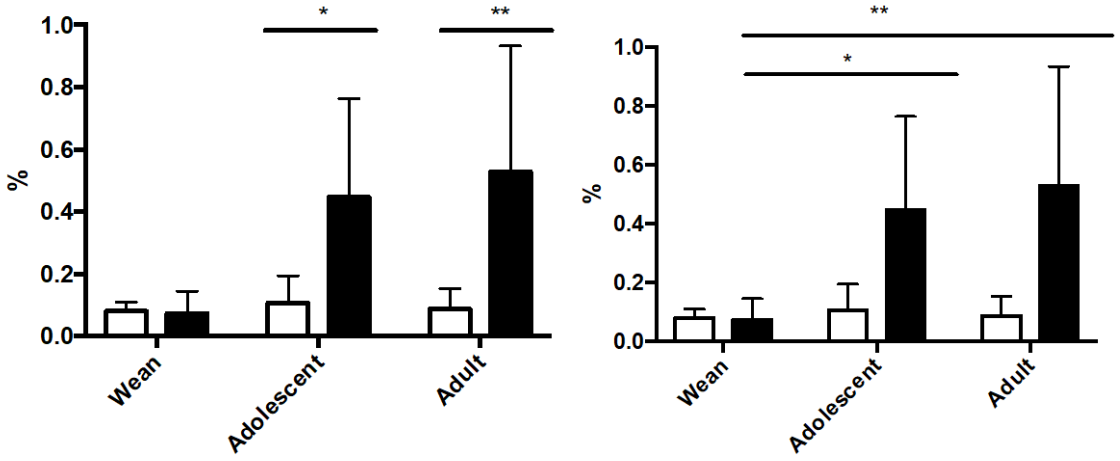

NCD

HFD

Detailed Statistical Analysis for Figure 16A

ANOVA table	**DF**	**F (DFn, DFd)**	**P value**
Interaction	2	F (2, 27) = 1.975	P=0.1583
Row Factor	2	F (2, 27) = 2.177	P=0.1329
Column Factor	1	F (1, 27) = 5.767	P=0.0235
Residual	27		

Tukey's multiple comparisons test	**Adjusted P Value**
Wean:NCD vs. Wean:HFD	>0.9999
Wean:NCD vs. Adolescent:NCD	>0.9999
Wean:NCD vs. Adolescent:HFD	0.1942
Wean:NCD vs. Adult:NCD	0.9784
Wean:NCD vs. Adult:HFD	0.9842
Wean:HFD vs. Adolescent:NCD	>0.9999
Wean:HFD vs. Adolescent:HFD	0.1758
Wean:HFD vs. Adult:NCD	0.9857
Wean:HFD vs. Adult:HFD	0.9776
Adolescent:NCD vs. Adolescent:HFD	0.0582
Adolescent:NCD vs. Adult:NCD	0.9828
Adolescent:NCD vs. Adult:HFD	0.9254
Adolescent:HFD vs. Adult:NCD	0.0192
Adolescent:HFD vs. Adult:HFD	0.5271
Adult:NCD vs. Adult:HFD	0.6766

Detailed Statistical Analysis for Figure 16B

ANOVA table	**DF**	**F (DFn, DFd)**	**P value**
Interaction	2	F (2, 27) = 3.07	P=0.0629
Row Factor	2	F (2, 27) = 2.912	P=0.0716
Column Factor	1	F (1, 27) = 6.158	P=0.0196
Residual	27		

Tukey's multiple comparisons test	Adjusted P Value
Wean:NCD vs. Wean:HFD	0.9969
Wean:NCD vs. Adolescent:NCD	>0.9999
Wean:NCD vs. Adolescent:HFD	0.69
Wean:NCD vs. Adult:NCD	>0.9999
Wean:NCD vs. Adult:HFD	0.0948
Wean:HFD vs. Adolescent:NCD	0.9979
Wean:HFD vs. Adolescent:HFD	0.4069
Wean:HFD vs. Adult:NCD	0.996
Wean:HFD vs. Adult:HFD	0.0342
Adolescent:NCD vs. Adolescent:HFD	0.458
Adolescent:NCD vs. Adult:NCD	>0.9999
Adolescent:NCD vs. Adult:HFD	0.0246
Adolescent:HFD vs. Adult:NCD	0.5222
Adolescent:HFD vs. Adult:HFD	0.7811
Adult:NCD vs. Adult:HFD	0.0337

Detailed Statistical Analysis for Figure 16C

ANOVA table	DF	F (DFn, DFd)	P value
Interaction	2	F (2, 27) = 3.666	P=0.0390
Row Factor	2	F (2, 27) = 4.12	P=0.0274
Column Factor	1	F (1, 27) = 14.53	P=0.0007
Residual	27		

Tukey's multiple comparisons test	Adjusted P Value
Wean:NCD vs. Wean:HFD	>0.9999
Wean:NCD vs. Adolescent:NCD	0.9999
Wean:NCD vs. Adolescent:HFD	0.0826
Wean:NCD vs. Adult:NCD	>0.9999
Wean:NCD vs. Adult:HFD	0.0197
Wean:HFD vs. Adolescent:NCD	0.9996
Wean:HFD vs. Adolescent:HFD	0.0734
Wean:HFD vs. Adult:NCD	>0.9999
Wean:HFD vs. Adult:HFD	0.0173

Tukey's multiple comparisons test	Adjusted P Value
Adolescent:NCD vs. Adolescent:HFD	0.0469
Adolescent:NCD vs. Adult:NCD	>0.9999
Adolescent:NCD vs. Adult:HFD	0.0079
Adolescent:HFD vs. Adult:NCD	0.0355
Adolescent:HFD vs. Adult:HFD	0.9871
Adult:NCD vs. Adult:HFD	0.006

Figure 16: γδ IELs from obese adolescent and adult mice produce increased amounts of the proinflammatory type cytokine, TNF-α.

Epithelial cells isolated from the small intestine of weanling (NCD n= 4, HFD n=4), adolescent (NCD n= 9, HFD n=4), and adult (NCD n= 8, HFD n=4) cohort of mice after 7 week HFD or NCD treatment. Epithelial cells were stained for CD3, γδ, CD8α T cells and intracellular cytokine, TNF-α. Percentages of cells producing TNF α from the (A) live CD3+ T cells (B) γδ T cells, and (C) CD8α γδ T cells as analyzed by flow cytometry. Figures (B) and (C) show duplicate figures to show significance between the cohorts and between the treatment groups. Two-way ANOVA was conducted using Prism Graph Pad software. * represents significant P value less than <0.05, and ** represents significant P value equal to or less than <0.01. Error bars represent SD.

A) αβ T cells producing TNF-α **B) CD4 T cells producing TNF-α**

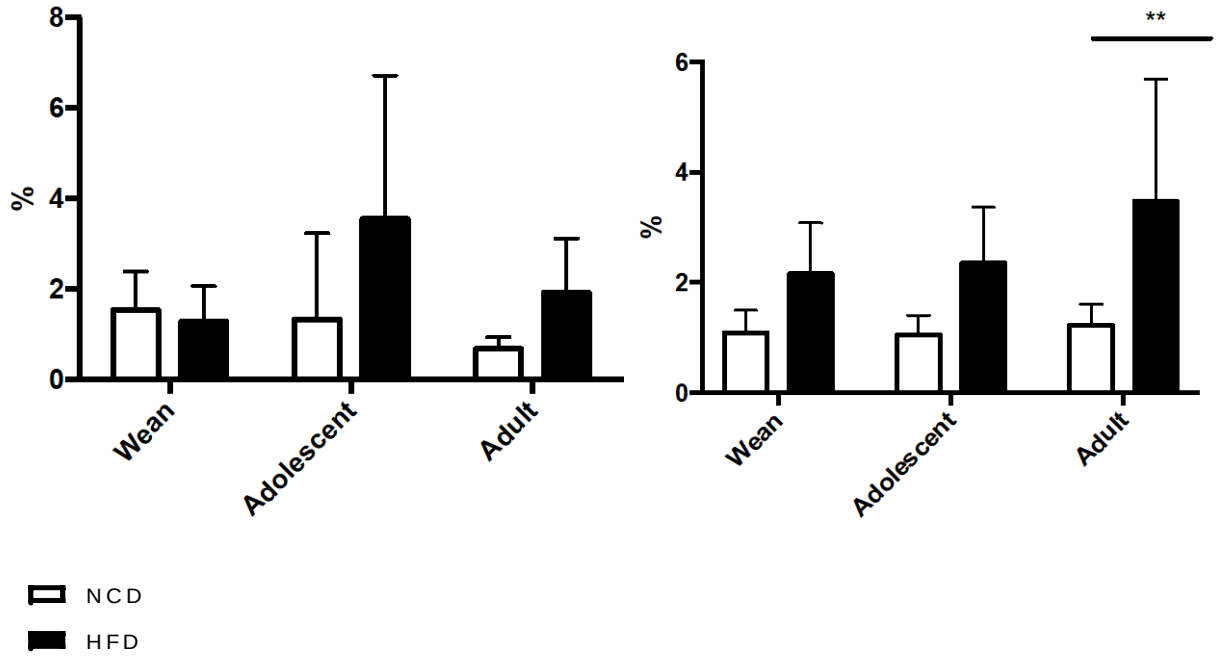

Detailed Statistical Analysis for Figure 17A

ANOVA table	DF	F (DFn, DFd)	P value
Interaction	2	F (2, 27) = 1.403	P=0.2631
Row Factor	2	F (2, 27) = 1.644	P=0.2120
Column Factor	1	F (1, 27) = 3.306	P=0.0801
Residual	27		

Tukey's multiple comparisons test	Adjusted P Value
Wean:NCD vs. Wean:HFD	>0.9999
Wean:NCD vs. Adolescent:NCD	>0.9999
Wean:NCD vs. Adolescent:HFD	0.4863
Wean:NCD vs. Adult:NCD	0.9496
Wean:NCD vs. Adult:HFD	0.9993
Wean:HFD vs. Adolescent:NCD	>0.9999
Wean:HFD vs. Adolescent:HFD	0.361
Wean:HFD vs. Adult:NCD	0.9886
Wean:HFD vs. Adult:HFD	0.9925

Tukey's multiple comparisons test	Adjusted P Value
Adolescent:NCD vs. Adolescent:HFD	0.2182
Adolescent:NCD vs. Adult:NCD	0.9586
Adolescent:NCD vs. Adult:HFD	0.9883
Adolescent:HFD vs. Adult:NCD	0.0649
Adolescent:HFD vs. Adult:HFD	0.6982
Adult:NCD vs. Adult:HFD	0.7972

Detailed Statistical Analysis for Figure 17B

ANOVA table	DF	F (DFn, DFd)	P value
Interaction	2	F (2, 27) = 1.148	P=0.3322
Row Factor	2	F (2, 27) = 1.9	P=0.1691
Column Factor	1	F (1, 27) = 20.44	P=0.0001
Residual	27		

Tukey's multiple comparisons test	Adjusted P Value
Wean:NCD vs. Wean:HFD	0.5782
Wean:NCD vs. Adolescent:NCD	>0.9999
Wean:NCD vs. Adolescent:HFD	0.3984
Wean:NCD vs. Adult:NCD	0.9999
Wean:NCD vs. Adult:HFD	0.012
Wean:HFD vs. Adolescent:NCD	0.3682
Wean:HFD vs. Adolescent:HFD	0.9996
Wean:HFD vs. Adult:NCD	0.5712
Wean:HFD vs. Adult:HFD	0.3526
Adolescent:NCD vs. Adolescent:HFD	0.2081
Adolescent:NCD vs. Adult:NCD	0.9987
Adolescent:NCD vs. Adult:HFD	0.002
Adolescent:HFD vs. Adult:NCD	0.367
Adolescent:HFD vs. Adult:HFD	0.5256
Adult:NCD vs. Adult:HFD	0.0053

Figure 17: CD4+ αβ IELs from obese adolescent and adult mice produce increased amounts of the proinflammatory type cytokine, TNFα.

Epithelial cells isolated from the small intestine of weanling (NCD n= 4, HFD n=4), adolescent (NCD n= 9, HFD n=4), and adult (NCD n= 8, HFD n=4) cohort of mice after 7 week HFD or NCD treatment. Epithelial cells were stained for CD3, αβ, CD4 T cells and the cytokine, TNF-α. Percentage of cells producing TNF α from (A) αβ T cells and (B) CD4+ αβ T cells as analyzed by flow cytometry. Two-way ANOVA was conducted using Prism Graph Pad software. *represents significant P value less than <0.05, and ** represents significant P value equal to or less than <0.01. Error bars represent SD.

A) CD3 T cells producing IFN-γ

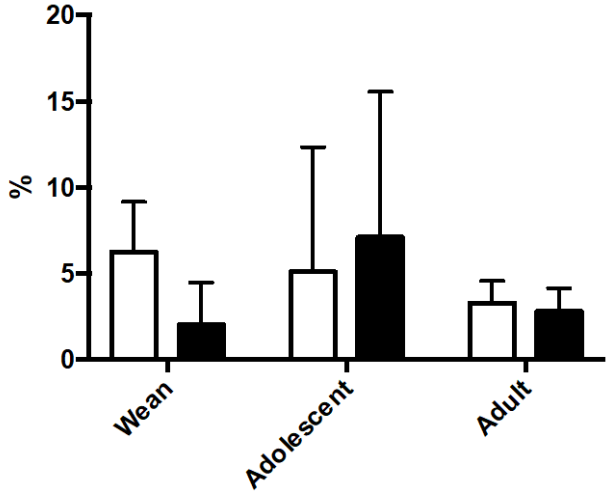

B) γδ T cells producing IFN-γ

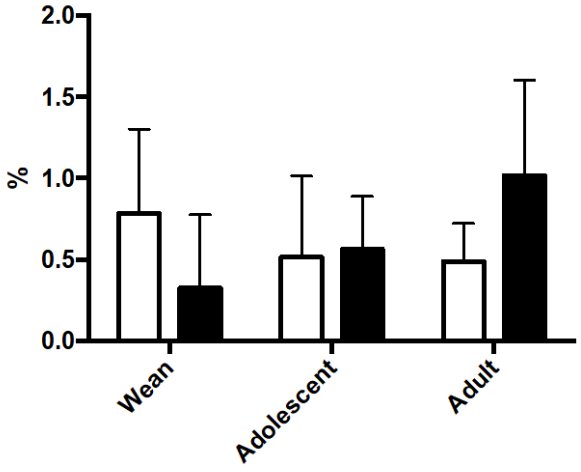

C) CD8α T cells producing IFN-γ

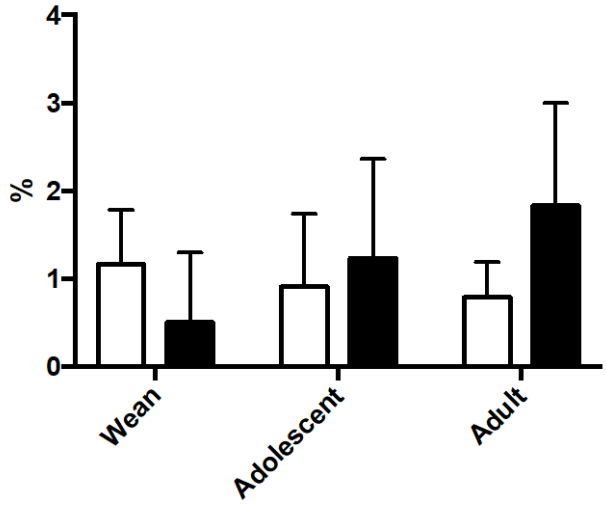

Detailed Statistical Analysis for Figure 18A

ANOVA table	**DF**	**F (DFn, DFd)**	**P value**
Interaction	2	F (2, 27) = 0.887	P=0.4235
Row Factor	2	F (2, 27) = 1.011	P=0.3771
Column Factor	1	F (1, 27) = 0.2305	P=0.6350
Residual	27		

Tukey's multiple comparisons test	Adjusted P Value
Wean:NCD vs. Wean:HFD	0.8408
Wean:NCD vs. Adolescent:NCD	0.9988
Wean:NCD vs. Adolescent:HFD	0.9999
Wean:NCD vs. Adult:NCD	0.9269
Wean:NCD vs. Adult:HFD	0.9248
Wean:HFD vs. Adolescent:NCD	0.9115
Wean:HFD vs. Adolescent:HFD	0.715
Wean:HFD vs. Adult:NCD	0.9984
Wean:HFD vs. Adult:HFD	>0.9999
Adolescent:NCD vs. Adolescent:HFD	0.9845
Adolescent:NCD vs. Adult:NCD	0.9762
Adolescent:NCD vs. Adult:HFD	0.9733
Adolescent:HFD vs. Adult:NCD	0.8176
Adolescent:HFD vs. Adult:HFD	0.8319
Adult:NCD vs. Adult:HFD	>0.9999

Detailed Statistical Analysis for Figure 18B

ANOVA table	DF	F (DFn, DFd)	P value
Interaction	2	F (2, 27) = 2.942	P=0.0699
Row Factor	2	F (2, 27) = 0.7796	P=0.4686
Column Factor	1	F (1, 27) = 0.06097	P=0.8068
Residual	27		

Tukey's multiple comparisons test	Adjusted P Value
Wean:NCD vs. Wean:HFD	0.6761
Wean:NCD vs. Adolescent:NCD	0.9053
Wean:NCD vs. Adolescent:HFD	0.9787
Wean:NCD vs. Adult:NCD	0.8759
Wean:NCD vs. Adult:HFD	0.9719
Wean:HFD vs. Adolescent:NCD	0.9774
Wean:HFD vs. Adolescent:HFD	0.9699
Wean:HFD vs. Adult:NCD	0.9892

Tukey's multiple comparisons test	Adjusted P Value
Wean:HFD vs. Adult:HFD	0.2509
Adolescent:NCD vs. Adolescent:HFD	>0.9999
Adolescent:NCD vs. Adult:NCD	>0.9999
Adolescent:NCD vs. Adult:HFD	0.4124
Adolescent:HFD vs. Adult:NCD	0.9997
Adolescent:HFD vs. Adult:HFD	0.6833
Adult:NCD vs. Adult:HFD	0.3787

Detailed Statistical Analysis for Figure 18C

ANOVA table	DF	F (DFn, DFd)	P value
Interaction	2	F (2, 27) = 2.535	P=0.0979
Row Factor	2	F (2, 27) = 0.8012	P=0.4592
Column Factor	1	F (1, 27) = 0.6226	P=0.4370
Residual	27		

Tukey's multiple comparisons test	Adjusted P Value
Wean:NCD vs. Wean:HFD	0.8538
Wean:NCD vs. Adolescent:NCD	0.9943
Wean:NCD vs. Adolescent:HFD	>0.9999
Wean:NCD vs. Adult:NCD	0.9723
Wean:NCD vs. Adult:HFD	0.8478
Wean:HFD vs. Adolescent:NCD	0.9599
Wean:HFD vs. Adolescent:HFD	0.7961
Wean:HFD vs. Adult:NCD	0.9918
Wean:HFD vs. Adult:HFD	0.2198
Adolescent:NCD vs. Adolescent:HFD	0.9836
Adolescent:NCD vs. Adult:NCD	0.9997
Adolescent:NCD vs. Adult:HFD	0.42
Adolescent:HFD vs. Adult:NCD	0.9444
Adolescent:HFD vs. Adult:HFD	0.8969
Adult:NCD vs. Adult:HFD	0.3141

Figure 18: No statistical change in IFN-γ production by γδ T cells from weanling, adolescent or adult cohorts.

Epithelial cells isolated from the small intestine of weanling (NCD n= 4, HFD n=4), adolescent (NCD n= 9, HFD n=4), and adult (NCD n= 8, HFD n=4) cohort of mice after 7 week HFD or NCD treatment. Epithelial cells isolated from the small intestine were stained for CD3, γδ, CD4 T cells and intracellular cytokine, IFN-γ. Percentages of cells producing IFN-γ from (A) live CD3+ T cells, (B) γδ T cells, and (C) CD8α γδ T cells as analyzed by flow cytometry. Two-way ANOVA was conducted using Prism Graph Pad software. * represents significant P value less than <0.05, and ** represents significant P value equal to or less than <0.01. Error bars represent SD.

A) αβ T cells producing IFN-γ

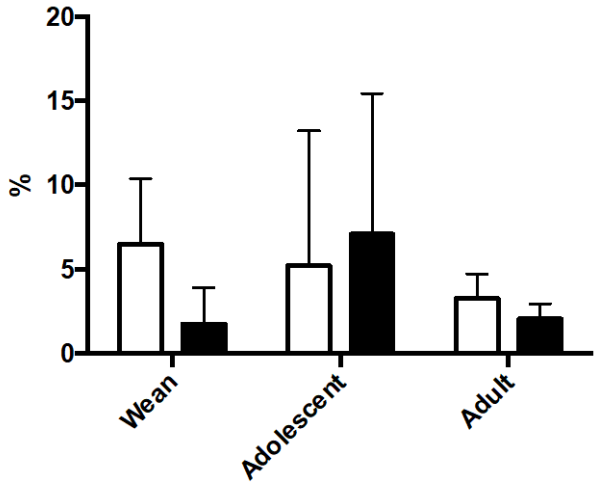

B) CD4 producing IFN-γ T cells

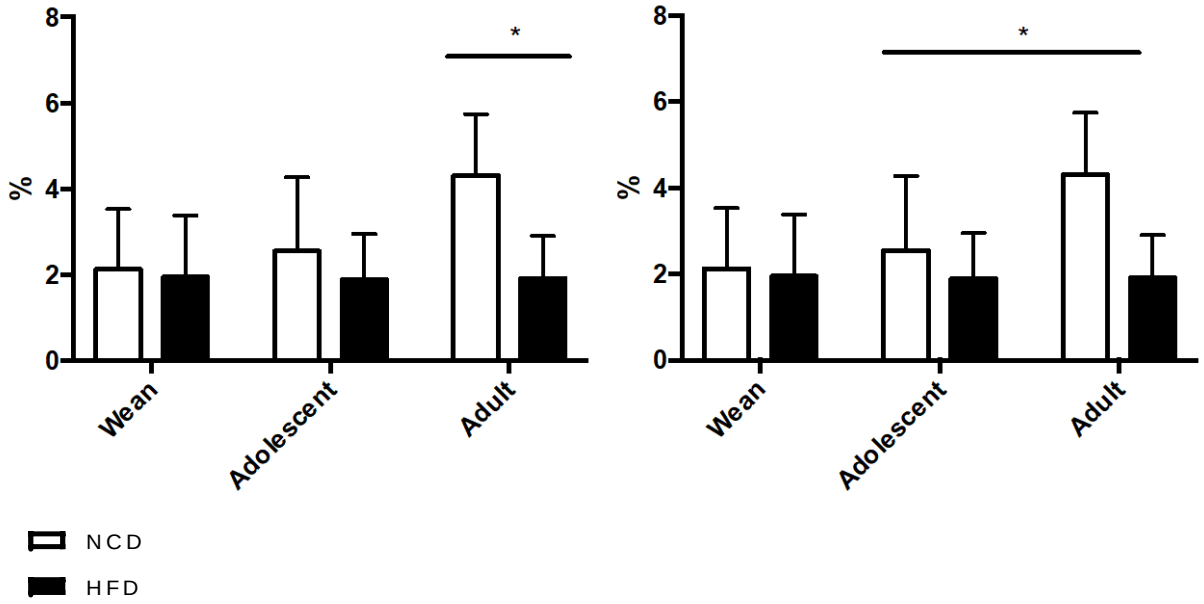

Detailed Statistical Analysis for Figure 19A

ANOVA table	DF	F (DFn, DFd)	P value
Interaction	2	F (2, 27) = 0.8546	P=0.4366
Row Factor	2	F (2, 27) = 1.136	P=0.3360
Column Factor	1	F (1, 27) = 0.4515	P=0.5073
Residual	27		

Tukey's multiple comparisons test	Adjusted P Value
Wean:NCD vs. Wean:HFD	0.8198
Wean:NCD vs. Adolescent:NCD	0.9987
Wean:NCD vs. Adolescent:HFD	>0.9999
Wean:NCD vs. Adult:NCD	0.9239
Wean:NCD vs. Adult:HFD	0.8542
Wean:HFD vs. Adolescent:NCD	0.8937
Wean:HFD vs. Adolescent:HFD	0.7357
Wean:HFD vs. Adult:NCD	0.9975
Wean:HFD vs. Adult:HFD	>0.9999
Adolescent:NCD vs. Adolescent:HFD	0.9921
Adolescent:NCD vs. Adult:NCD	0.9746
Adolescent:NCD vs. Adult:HFD	0.9232
Adolescent:HFD vs. Adult:NCD	0.8559
Adolescent:HFD vs. Adult:HFD	0.7767
Adult:NCD vs. Adult:HFD	0.9991

Detailed Statistical Analysis for Figure 19B

ANOVA table	DF	F (DFn, DFd)	P value
Interaction	2	F (2, 27) = 1.609	P=0.2187
Row Factor	2	F (2, 27) = 1.58	P=0.2244
Column Factor	1	F (1, 27) = 4.047	P=0.0543
Residual	27		

Tukey's multiple comparisons test	Adjusted P Value
Wean:NCD vs. Wean:HFD	>0.9999
Wean:NCD vs. Adolescent:NCD	0.9962
Wean:NCD vs. Adolescent:HFD	>0.9999
Wean:NCD vs. Adult:NCD	0.168
Wean:NCD vs. Adult:HFD	>0.9999
Wean:HFD vs. Adolescent:NCD	0.9813
Wean:HFD vs. Adolescent:HFD	>0.9999
Wean:HFD vs. Adult:NCD	0.1144
Wean:HFD vs. Adult:HFD	>0.9999

Tukey's multiple comparisons test	Adjusted P Value
Adolescent:NCD vs. Adolescent:HFD	0.9723
Adolescent:NCD vs. Adult:NCD	0.1562
Adolescent:NCD vs. Adult:HFD	0.9763
Adolescent:HFD vs. Adult:NCD	0.1005
Adolescent:HFD vs. Adult:HFD	>0.9999
Adult:NCD vs. Adult:HFD	0.106

Figure 19: Obesity results in reduced IFN-γ production by CD4 T cells in adult mice.

Epithelial cells isolated from the small intestine of weanling (NCD n= 4, HFD n=4), adolescent (NCD n= 9, HFD n=4), and adult (NCD n= 8, HFD n=4) cohort of mice after 7 week HFD or NCD treatment. Epithelial cells were stained for CD3, αβ, CD4 T cells and intracellular cytokine, IFN-γ. Percentage of cells producing IFN-γ (A) from αβ T cells and (B) CD4+ αβ T cells as analyzed by flow cytometry. Figure (B) shows duplicate figures to show significance between the cohorts and between the treatment groups. Two-way ANOVA was conducted using Prism Graph Pad software. * represents significant P value less than <0.05, and ** represents significant P value equal to or less than <0.01. Error bars represent SD.

References

Jeffery Jensen Arnett. (2012). *Adolescent Psychology Around the World*. Taylor & Francis. Retrieved from https://books.google.com/books?id=QJB5AgAAQBAJ

Berg, A. H., & Scherer, P. E. (2005). Adipose tissue, inflammation, and cardiovascular disease. *Circulation Research*, *96*(9), 939–949. https://doi.org/10.1161/01.RES.0000163635.62927.34

Binkley, P. F., Murray, K. D., Watson, K. M., Myerowitz, P. D., & Leier, C. V. (1991). Dobutamine increases cardiac output of the total artificial heart. Implications for vascular contribution of inotropic agents to augmented ventricular function. *Circulation*, *84*(3), 1210–1215.

Blain, A., Cattan, S., Beaugerie, L., Carbonnel, F., Gendre, J. P., & Cosnes, J. (2002). Crohn's disease clinical course and severity in obese patients. *Clinical Nutrition*, *21*(1), 51–57. https://doi.org/10.1054/clnu.2001.0503

Blakytny, R., & Jude, E. (2006). The molecular biology of chronic wounds and delayed healing in diabetes. *Diabetic Medicine*, *23*(6), 594–608. https://doi.org/10.1111/j.1464-5491.2006.01773.x

Boismenu, R., & Havran, W. L. (1994). Modulation of epithelial cell growth by intraepithelial gamma delta T cells. *Science (New York, N.Y.)*, *266*(5188), 1253–1255.

Bonneville, M., O'Brien, R. L., & Born, W. K. (2010). Gammadelta T cell effector functions: a blend of innate programming and acquired plasticity. *Nature Reviews. Immunology*, *10*(7), 467–478. https://doi.org/10.1038/nri2781

Brandes, M., Willimann, K., Lang, A. B., Nam, K.-H., Jin, C., Brenner, M. B., … Moser, B. (2003). Flexible migration program regulates gamma delta T-cell involvement in humoral immunity. *Blood*, *102*(10), 3693–3701. https://doi.org/10.1182/blood-2003-04-1016

Brophy, S., Cooksey, R., Gravenor, M. B., Mistry, R., Thomas, N., Lyons, R. A., & Williams, R. (2009). Risk factors for childhood obesity at age 5: analysis of the millennium cohort study. *BMC Public Health*, *9*, 467. https://doi.org/10.1186/1471-2458-9-467

Brown, D. R., Carroll, D. D., Workman, L. M., Carlson, S. A., & Brown, D. W. (2014). Physical activity and health-related quality of life: US adults with and without limitations. *Quality of Life Research: An International Journal of Quality of Life Aspects of Treatment, Care and Rehabilitation*, *23*(10), 2673–2680. https://doi.org/10.1007/s11136-014-0739-z

Brun, P., Castagliuolo, I., Di Leo, V., Buda, A., Pinzani, M., Palù, G., & Martines, D. (2007). Increased intestinal permeability in obese mice: new evidence in the pathogenesis of nonalcoholic steatohepatitis. *American Journal of Physiology. Gastrointestinal and Liver Physiology*, *292*(2), G518–525. https://doi.org/10.1152/ajpgi.00024.2006

Buettner, R., Schölmerich, J., & Bollheimer, L. C. (2007). High-fat diets: modeling the metabolic disorders of human obesity in rodents. *Obesity (Silver Spring, Md.)*, *15*(4), 798–808. https://doi.org/10.1038/oby.2007.608

Cani, P. D., Bibiloni, R., Knauf, C., Waget, A., Neyrinck, A. M., Delzenne, N. M., & Burcelin, R. (2008). Changes in gut microbiota control metabolic endotoxemia-induced inflammation in high-fat diet-induced obesity and diabetes in mice. *Diabetes*, *57*(6), 1470–1481. https://doi.org/10.2337/db07-1403

Chen, W., Jin, W., Hardegen, N., Lei, K.-J., Li, L., Marinos, N., … Wahl, S. M. (2003). Conversion of peripheral CD4+CD25- naive T cells to CD4+CD25+ regulatory T cells by TGF-beta induction of transcription factor Foxp3. *The Journal of Experimental Medicine*, *198*(12), 1875–1886. https://doi.org/10.1084/jem.20030152

Chen, Y., Chou, K., Fuchs, E., Havran, W. L., & Boismenu, R. (2002). Protection of the intestinal mucosa by intraepithelial gamma delta T cells. *Proceedings of the National Academy of Sciences of the United States of America*, *99*(22), 14338–14343. https://doi.org/10.1073/pnas.212290499

Cheroutre, H., & Lambolez, F. (2008). The thymus chapter in the life of gut-specific intra epithelial lymphocytes. *Current Opinion in Immunology*, *20*(2), 185–191. https://doi.org/10.1016/j.coi.2008.03.009

Cheroutre, H., Lambolez, F., & Mucida, D. (2011). The light and dark sides of intestinal intraepithelial lymphocytes. *Nature Reviews. Immunology*, *11*(7), 445–456. https://doi.org/10.1038/nri3007

Cheung, K. P., Taylor, K. R., & Jameson, J. M. (2012). Immunomodulation at epithelial sites by obesity and metabolic disease. *Immunologic Research*, *52*(3), 182–199. https://doi.org/10.1007/s12026-011-8261-7

Clark, J., Vagenas, P., Panesar, M., & Cope, A. P. (2005). What does tumour necrosis factor excess do to the immune system long term? *Annals of the Rheumatic Diseases*, *64 Suppl 4*, iv70–76. https://doi.org/10.1136/ard.2005.042523

Dalton, J. E., Cruickshank, S. M., Egan, C. E., Mears, R., Newton, D. J., Andrew, E. M., … Carding, S. R. (2006). Intraepithelial gammadelta+ lymphocytes maintain the integrity of intestinal epithelial tight junctions in response to infection. *Gastroenterology*, *131*(3), 818–829. https://doi.org/10.1053/j.gastro.2006.06.003

Dandekar, S., George, M. D., & Bäumler, A. J. (2010). Th17 cells, HIV and the gut mucosal barrier. *Current Opinion in HIV and AIDS*, *5*(2), 173–178. https://doi.org/10.1097/COH.0b013e328335eda3

de La Serre, C. B., Ellis, C. L., Lee, J., Hartman, A. L., Rutledge, J. C., & Raybould, H. E. (2010). Propensity to high-fat diet-induced obesity in rats is associated with changes in the gut microbiota and gut inflammation. *American Journal of Physiology. Gastrointestinal and Liver Physiology*, *299*(2), G440–448. https://doi.org/10.1152/ajpgi.00098.2010

Dharakul, T., Labbe, M., Cohen, J., Bellamy, A. R., Street, J. E., Mackow, E. R., … Greenberg, H. B. (1991). Immunization with baculovirus-expressed recombinant rotavirus proteins VP1, VP4, VP6, and VP7 induces CD8+ T lymphocytes that mediate clearance of chronic rotavirus infection in SCID mice. *Journal of Virology*, *65*(11), 5928–5932.

Ding, S., Chi, M. M., Scull, B. P., Rigby, R., Schwerbrock, N. M. J., Magness, S., … Lund, P. K. (2010). High-fat diet: bacteria interactions promote intestinal inflammation which precedes and correlates with obesity and insulin resistance in mouse. *PloS One*, *5*(8), e12191. https://doi.org/10.1371/journal.pone.0012191

Duffaut, C., Zakaroff-Girard, A., Bourlier, V., Decaunes, P., Maumus, M., Chiotasso, P., … Bouloumié, A. (2009). Interplay between human adipocytes and T lymphocytes in obesity:

CCL20 as an adipochemokine and T lymphocytes as lipogenic modulators. *Arteriosclerosis, Thrombosis, and Vascular Biology*, *29*(10), 1608–1614. https://doi.org/10.1161/ATVBAHA.109.192583

Dutta, S., & Sengupta, P. (2016). Men and mice: Relating their ages. *Life Sciences*, *152*, 244–248. https://doi.org/10.1016/j.lfs.2015.10.025

Eberl, M., Roberts, G. W., Meuter, S., Williams, J. D., Topley, N., & Moser, B. (2009). A rapid crosstalk of human gammadelta T cells and monocytes drives the acute inflammation in bacterial infections. *PLoS Pathogens*, *5*(2), e1000308. https://doi.org/10.1371/journal.ppat.1000308

Edelblum, K. L., Shen, L., Weber, C. R., Marchiando, A. M., Clay, B. S., Wang, Y., … Turner, J. R. (2012). Dynamic migration of γδ intraepithelial lymphocytes requires occludin. *Proceedings of the National Academy of Sciences of the United States of America*, *109*(18), 7097–7102. https://doi.org/10.1073/pnas.1112519109

Edelblum, K. L., & Turner, J. R. (2009). The tight junction in inflammatory disease: communication breakdown. *Current Opinion in Pharmacology*, *9*(6), 715–720. https://doi.org/10.1016/j.coph.2009.06.022

Egan, C. E., Dalton, J. E., Andrew, E. M., Smith, J. E., Gubbels, M.-J., Striepen, B., & Carding, S. R. (2005). A requirement for the Vgamma1+ subset of peripheral gammadelta T cells in the control of the systemic growth of Toxoplasma gondii and infection-induced pathology. *Journal of Immunology (Baltimore, Md.: 1950)*, *175*(12), 8191–8199.

Epple, H.-J., Allers, K., Tröger, H., Kühl, A., Erben, U., Fromm, M., … Schneider, T. (2010). Acute HIV infection induces mucosal infiltration with CD4+ and CD8+ T cells, epithelial apoptosis, and a mucosal barrier defect. *Gastroenterology*, *139*(4), 1289–1300. https://doi.org/10.1053/j.gastro.2010.06.065

Fahrer, A. M., Konigshofer, Y., Kerr, E. M., Ghandour, G., Mack, D. H., Davis, M. M., & Chien, Y. H. (2001). Attributes of gammadelta intraepithelial lymphocytes as suggested by their transcriptional profile. *Proceedings of the National Academy of Sciences of the United States of America*, *98*(18), 10261–10266. https://doi.org/10.1073/pnas.171320798

Fain, J. N., Madan, A. K., Hiler, M. L., Cheema, P., & Bahouth, S. W. (2004). Comparison of the release of adipokines by adipose tissue, adipose tissue matrix, and adipocytes from visceral and subcutaneous abdominal adipose tissues of obese humans. *Endocrinology*, *145*(5), 2273–2282. https://doi.org/10.1210/en.2003-1336

Farah, C. S., Kermode, J. A., Downie, S. R., Brown, N. J., Hardaker, K. M., Berend, N., … Salome, C. M. (2011). Obesity is a determinant of asthma control independent of inflammation and lung mechanics. *Chest*, *140*(3), 659–666. https://doi.org/10.1378/chest.11-0027

Feczkó, J., Pestessy, J., & Harmath, Z. (1976). [Isolated luxation of the trapezium bone]. *Magyar Traumatológia, Orthopaedia És Helyreállító Sebészet*, *19*(1), 65–68.

Feuerer, M., Herrero, L., Cipolletta, D., Naaz, A., Wong, J., Nayer, A., … Mathis, D. (2009). Lean, but not obese, fat is enriched for a unique population of regulatory T cells that affect metabolic parameters. *Nature Medicine*, *15*(8), 930–939. https://doi.org/10.1038/nm.2002

Finkelstein, E. A., Trogdon, J. G., Cohen, J. W., & Dietz, W. (2009). Annual medical spending attributable to obesity: payer-and service-specific estimates. *Health Affairs (Project Hope)*, *28*(5), w822–831. https://doi.org/10.1377/hlthaff.28.5.w822

Flegal, K. M., Carroll, M. D., Ogden, C. L., & Johnson, C. L. (2002). Prevalence and trends in obesity among US adults, 1999-2000. *JAMA*, *288*(14), 1723–1727.

Flück, K., Breves, G., Fandrey, J., & Winning, S. (2015). Hypoxia-inducible factor 1 in dendritic cells is crucial for the activation of protective regulatory T cells in murine colitis. *Mucosal Immunology*. https://doi.org/10.1038/mi.2015.67

Fox, J. G. (Ed.). (2007). *The mouse in biomedical research* (2nd ed). Amsterdam ; Boston: Elsevier, AP.

Gangadharan, D., Lambolez, F., Attinger, A., Wang-Zhu, Y., Sullivan, B. A., & Cheroutre, H. (2006). Identification of pre- and postselection TCRalphabeta+ intraepithelial lymphocyte precursors in the thymus. *Immunity*, *25*(4), 631–641. https://doi.org/10.1016/j.immuni.2006.08.018

García, V. E., Jullien, D., Song, M., Uyemura, K., Shuai, K., Morita, C. T., & Modlin, R. L. (1998). IL-15 enhances the response of human gamma delta T cells to nonpeptide [correction of nonpetide] microbial antigens. *Journal of Immunology (Baltimore, Md.: 1950)*, *160*(9), 4322–4329.

Giacomelli, R., Parzanese, I., Frieri, G., Passacantando, A., Pizzuto, F., Pimpo, T., … Tonietti, G. (1994). Increase of circulating gamma/delta T lymphocytes in the peripheral blood of patients affected by active inflammatory bowel disease. *Clinical and Experimental Immunology*, *98*(1), 83–88.

Girardi, M. (2006). Immunosurveillance and immunoregulation by gammadelta T cells. *The Journal of Investigative Dermatology*, *126*(1), 25–31. https://doi.org/10.1038/sj.jid.5700003

Greenberg, A. S., & Obin, M. S. (2006). Obesity and the role of adipose tissue in inflammation and metabolism. *The American Journal of Clinical Nutrition*, *83*(2), 461S–465S.

Guida, B., Nino, M., Perrino, N. R., Laccetti, R., Trio, R., Labella, S., & Balato, N. (2010). The impact of obesity on skin disease and epidermal permeability barrier status. *Journal of the European Academy of Dermatology and Venereology: JEADV*, *24*(2), 191–195. https://doi.org/10.1111/j.1468-3083.2009.03503.x

Hahm, K. B., Im, Y. H., Parks, T. W., Park, S. H., Markowitz, S., Jung, H. Y., … Kim, S. J. (2001). Loss of transforming growth factor beta signalling in the intestine contributes to tissue injury in inflammatory bowel disease. *Gut*, *49*(2), 190–198.

Halle, M., Korsten-Reck, U., Wolfarth, B., & Berg, A. (2004). Low-grade systemic inflammation in overweight children: impact of physical fitness. *Exercise Immunology Review*, *10*, 66–74.

Hamada, S., Umemura, M., Shiono, T., Hara, H., Kishihara, K., Tanaka, K., … Matsuzaki, G. (2008). Importance of murine Vdelta1gammadelta T cells expressing interferon-gamma and interleukin-17A in innate protection against Listeria monocytogenes infection. *Immunology*, *125*(2), 170–177. https://doi.org/10.1111/j.1365-2567.2008.02841.x

Hansen, S. G., Vieville, C., Whizin, N., Coyne-Johnson, L., Siess, D. C., Drummond, D. D., … Picker, L. J. (2009). Effector memory T cell responses are associated with protection of rhesus

monkeys from mucosal simian immunodeficiency virus challenge. *Nature Medicine*, *15*(3), 293–299. https://doi.org/10.1038/nm.1935

Hass, D. J., Brensinger, C. M., Lewis, J. D., & Lichtenstein, G. R. (2006). The impact of increased body mass index on the clinical course of Crohn's disease. *Clinical Gastroenterology and Hepatology: The Official Clinical Practice Journal of the American Gastroenterological Association*, *4*(4), 482–488. https://doi.org/10.1016/j.cgh.2005.12.015

Havran, W. L., & Allison, J. P. (1988). Developmentally ordered appearance of thymocytes expressing different T-cell antigen receptors. *Nature*, *335*(6189), 443–445. https://doi.org/10.1038/335443a0

Havran, W. L., & Allison, J. P. (1990). Origin of Thy-1+ dendritic epidermal cells of adult mice from fetal thymic precursors. *Nature*, *344*(6261), 68–70. https://doi.org/10.1038/344068a0

Havran, W. L., & Jameson, J. M. (2010). Epidermal T cells and wound healing. *Journal of Immunology (Baltimore, Md.: 1950)*, *184*(10), 5423–5428. https://doi.org/10.4049/jimmunol.0902733

Hayday, A., & Gibbons, D. (2008). Brokering the peace: the origin of intestinal T cells. *Mucosal Immunology*, *1*(3), 172–174. https://doi.org/10.1038/mi.2008.8

Hayes, E. K., Lechowicz, A., Petrik, J. J., Storozhuk, Y., Paez-Parent, S., Dai, Q., … Raha, S. (2012). Adverse fetal and neonatal outcomes associated with a life-long high fat diet: role of altered development of the placental vasculature. *PloS One*, *7*(3), e33370. https://doi.org/10.1371/journal.pone.0033370

Heerwagen, M. J. R., Miller, M. R., Barbour, L. A., & Friedman, J. E. (2010). Maternal obesity and fetal metabolic programming: a fertile epigenetic soil. *American Journal of Physiology. Regulatory, Integrative and Comparative Physiology*, *299*(3), R711–722. https://doi.org/10.1152/ajpregu.00310.2010

Hennessy, C. H., Moriarty, D. G., Zack, M. M., Scherr, P. A., & Brackbill, R. (1994). Measuring health-related quality of life for public health surveillance. *Public Health Reports (Washington, D.C.: 1974)*, *109*(5), 665–672.

Hernandez, L. L., Grayson, B. E., Yadav, E., Seeley, R. J., & Horseman, N. D. (2012). High fat diet alters lactation outcomes: possible involvement of inflammatory and serotonergic pathways. *PloS One*, *7*(3), e32598. https://doi.org/10.1371/journal.pone.0032598

Hill, J. O., Wyatt, H. R., & Peters, J. C. (2012). Energy balance and obesity. *Circulation*, *126*(1), 126–132. https://doi.org/10.1161/CIRCULATIONAHA.111.087213

Hjemdahl, P. (1976). [Seloken (Metoprolol, Hässle)]. *Läkartidningen*, *73*(12), 1092.

Horton, T. J., Drougas, H., Brachey, A., Reed, G. W., Peters, J. C., & Hill, J. O. (1995). Fat and carbohydrate overfeeding in humans: different effects on energy storage. *The American Journal of Clinical Nutrition*, *62*(1), 19–29.

Hüe, S., Mention, J.-J., Monteiro, R. C., Zhang, S., Cellier, C., Schmitz, J., … Caillat-Zucman, S. (2004). A direct role for NKG2D/MICA interaction in villous atrophy during celiac disease. *Immunity*, *21*(3), 367–377. https://doi.org/10.1016/j.immuni.2004.06.018

Inagaki-Ohara, K., Chinen, T., Matsuzaki, G., Sasaki, A., Sakamoto, Y., Hiromatsu, K., … Yoshimura, A. (2004). Mucosal T cells bearing TCRgammadelta play a protective role in intestinal inflammation. *Journal of Immunology (Baltimore, Md.: 1950)*, *173*(2), 1390–1398.

Ito, K., Bonneville, M., Takagaki, Y., Nakanishi, N., Kanagawa, O., Krecko, E. G., & Tonegawa, S. (1989). Different gamma delta T-cell receptors are expressed on thymocytes at different stages of development. *Proceedings of the National Academy of Sciences of the United States of America*, *86*(2), 631–635.

Jackson, I. J., & Abbott, C. M. (Eds.). (2000). *Mouse genetics and transgenics: a practical approach*. Oxford ; New York: Oxford University Press.

Jameson, J. M., Cauvi, G., Sharp, L. L., Witherden, D. A., & Havran, W. L. (2005). Gammadelta T cell-induced hyaluronan production by epithelial cells regulates inflammation. *The Journal of Experimental Medicine*, *201*(8), 1269–1279. https://doi.org/10.1084/jem.20042057

Jameson, J. M., Cauvi, G., Witherden, D. A., & Havran, W. L. (2004). A keratinocyte-responsive gamma delta TCR is necessary for dendritic epidermal T cell activation by damaged keratinocytes and maintenance in the epidermis. *Journal of Immunology (Baltimore, Md.: 1950)*, *172*(6), 3573–3579.

Jameson, J., Ugarte, K., Chen, N., Yachi, P., Fuchs, E., Boismenu, R., & Havran, W. L. (2002). A role for skin gammadelta T cells in wound repair. *Science (New York, N.Y.)*, *296*(5568), 747–749. https://doi.org/10.1126/science.1069639

Jarry, A., Cerf-Bensussan, N., Brousse, N., Selz, F., & Guy-Grand, D. (1990). Subsets of CD3+ (T cell receptor alpha/beta or gamma/delta) and CD3- lymphocytes isolated from normal human gut epithelium display phenotypical features different from their counterparts in peripheral blood. *European Journal of Immunology*, *20*(5), 1097–1103. https://doi.org/10.1002/eji.1830200523

Jeffery Jensen Arnett. (2012). *Adolescent Psychology Around the World*. Taylor & Francis. Retrieved from https://books.google.com/books?id=QJB5AgAAQBAJ

Johnson, A. M. F., & Olefsky, J. M. (2013). The origins and drivers of insulin resistance. *Cell*, *152*(4), 673–684. https://doi.org/10.1016/j.cell.2013.01.041

Jungheim, E. S., Schoeller, E. L., Marquard, K. L., Louden, E. D., Schaffer, J. E., & Moley, K. H. (2010). Diet-induced obesity model: abnormal oocytes and persistent growth abnormalities in the offspring. *Endocrinology*, *151*(8), 4039–4046. https://doi.org/10.1210/en.2010-0098

Kanwar, S. S., Ganguly, N. K., Walia, B. N., & Mahajan, R. C. (1986). Direct and antibody dependent cell mediated cytotoxicity against Giardia lamblia by splenic and intestinal lymphoid cells in mice. *Gut*, *27*(1), 73–77.

Kern, P. A., Ranganathan, S., Li, C., Wood, L., & Ranganathan, G. (2001). Adipose tissue tumor necrosis factor and interleukin-6 expression in human obesity and insulin resistance. *American Journal of Physiology. Endocrinology and Metabolism*, *280*(5), E745–751.

Koda, M., Sulkowska, M., Kanczuga-Koda, L., Cascio, S., Colucci, G., Russo, A., … Sulkowski, S. (2007). Expression of the obesity hormone leptin and its receptor correlates with hypoxia-inducible factor-1 alpha in human colorectal cancer. *Annals of Oncology: Official Journal of the*

European Society for Medical Oncology / ESMO, *18 Suppl 6*, vi116–119. https://doi.org/10.1093/annonc/mdm238

Koebnick, C., Black, M. H., Smith, N., Der-Sarkissian, J. K., Porter, A. H., Jacobsen, S. J., & Wu, J. J. (2011). The association of psoriasis and elevated blood lipids in overweight and obese children. *The Journal of Pediatrics*, *159*(4), 577–583. https://doi.org/10.1016/j.jpeds.2011.03.006

Kohyama, M., Hachimura, S., Nanno, M., Ishikawa, H., & Kaminogawa, S. (1997). Analysis of cytokine producing activity of intestinal intraepithelial T cells from TCR beta-chain and delta-chain mutant mice. *Microbiology and Immunology*, *41*(4), 353–359.

Komori, H. K., Witherden, D. A., Kelly, R., Sendaydiego, K., Jameson, J. M., Teyton, L., & Havran, W. L. (2012). Cutting edge: dendritic epidermal γδ T cell ligands are rapidly and locally expressed by keratinocytes following cutaneous wounding. *Journal of Immunology (Baltimore, Md.: 1950)*, *188*(7), 2972–2976. https://doi.org/10.4049/jimmunol.1100887

Kühl, A. A., Pawlowski, N. N., Grollich, K., Loddenkemper, C., Zeitz, M., & Hoffmann, J. C. (2007). Aggravation of intestinal inflammation by depletion/deficiency of gammadelta T cells in different types of IBD animal models. *Journal of Leukocyte Biology*, *81*(1), 168–175. https://doi.org/10.1189/jlb.1105696

Laroui, H., Ingersoll, S. A., Liu, H. C., Baker, M. T., Ayyadurai, S., Charania, M. A., … Merlin, D. (2012). Dextran sodium sulfate (DSS) induces colitis in mice by forming nano-lipocomplexes with medium-chain-length fatty acids in the colon. *PloS One*, *7*(3), e32084. https://doi.org/10.1371/journal.pone.0032084

Leandersson, K., Jaensson, E., & Ivars, F. (2006). T cells developing in fetal thymus of T-cell receptor alpha-chain transgenic mice colonize gammadelta T-cell-specific epithelial niches but lack long-term reconstituting potential. *Immunology*, *119*(1), 134–142. https://doi.org/10.1111/j.1365-2567.2006.02415.x

Lee, H.-C., Tomiyama, K., Ye, S.-K., Kawai, K., & Ikuta, K. (2002). Seeding of dendritic epidermal T cells in the neonatal skin is reduced in 129 strain of mice. *Immunology Letters*, *81*(3), 211–216.

Lee, Y.-H., & Pratley, R. E. (2005). The evolving role of inflammation in obesity and the metabolic syndrome. *Current Diabetes Reports*, *5*(1), 70–75.

Lepage, A. C., Buzoni-Gatel, D., Bout, D. T., & Kasper, L. H. (1998). Gut-derived intraepithelial lymphocytes induce long term immunity against Toxoplasma gondii. *Journal of Immunology (Baltimore, Md.: 1950)*, *161*(9), 4902–4908.

Lin, S., Thomas, T. C., Storlien, L. H., & Huang, X. F. (2000). Development of high fat diet-induced obesity and leptin resistance in C57Bl/6J mice. *International Journal of Obesity and Related Metabolic Disorders: Journal of the International Association for the Study of Obesity*, *24*(5), 639–646.

Li, Q., Duan, L., Estes, J. D., Ma, Z.-M., Rourke, T., Wang, Y., … Haase, A. T. (2005). Peak SIV replication in resting memory CD4+ T cells depletes gut lamina propria CD4+ T cells. *Nature*, *434*(7037), 1148–1152. https://doi.org/10.1038/nature03513

Li, Z., Zhang, C., Zhou, Z., Zhang, J., Zhang, J., & Tian, Z. (2012). Small Intestinal Intraepithelial Lymphocytes Expressing CD8 and T Cell Receptor Are Involved in Bacterial Clearance during Salmonella enterica Serovar Typhimurium Infection. *Infection and Immunity*, *80*(2), 565–574. https://doi.org/10.1128/IAI.05078-11

Löffler, H., Aramaki, J. U. N., & Effendy, I. (2002). The influence of body mass index on skin susceptibility to sodium lauryl sulphate. *Skin Research and Technology: Official Journal of International Society for Bioengineering and the Skin (ISBS) [and] International Society for Digital Imaging of Skin (ISDIS) [and] International Society for Skin Imaging (ISSI)*, *8*(1), 19–22.

Long, M. D., Crandall, W. V., Leibowitz, I. H., Duffy, L., del Rosario, F., Kim, S. C., … ImproveCareNow Collaborative for Pediatric IBD. (2011). Prevalence and epidemiology of overweight and obesity in children with inflammatory bowel disease. *Inflammatory Bowel Diseases*, *17*(10), 2162–2168. https://doi.org/10.1002/ibd.21585

Lundvall, J., & Järhult, J. (1976). Beta adrenergic dilator component of the sympathetic vascular response in skeletal muscle. Influence on the micro-circulation and on transcapillary exchange. *Acta Physiologica Scandinavica*, *96*(2), 180–192. https://doi.org/10.1111/j.1748-1716.1976.tb10187.x

Luzzo, K. M., Wang, Q., Purcell, S. H., Chi, M., Jimenez, P. T., Grindler, N., … Moley, K. H. (2012). High fat diet induced developmental defects in the mouse: oocyte meiotic aneuploidy and fetal growth retardation/brain defects. *PloS One*, *7*(11), e49217. https://doi.org/10.1371/journal.pone.0049217

MacLeod, A. S., Hemmers, S., Garijo, O., Chabod, M., Mowen, K., Witherden, D. A., & Havran, W. L. (2013). Dendritic epidermal T cells regulate skin antimicrobial barrier function. *The Journal of Clinical Investigation*, *123*(10), 4364–4374. https://doi.org/10.1172/JCI70064

McVay, L. D., Li, B., Biancaniello, R., Creighton, M. A., Bachwich, D., Lichtenstein, G., … Carding, S. R. (1997). Changes in human mucosal gamma delta T cell repertoire and function associated with the disease process in inflammatory bowel disease. *Molecular Medicine (Cambridge, Mass.)*, *3*(3), 183–203.

Mehandru, S., Poles, M. A., Tenner-Racz, K., Horowitz, A., Hurley, A., Hogan, C., … Markowitz, M. (2004). Primary HIV-1 infection is associated with preferential depletion of CD4+ T lymphocytes from effector sites in the gastrointestinal tract. *The Journal of Experimental Medicine*, *200*(6), 761–770. https://doi.org/10.1084/jem.20041196

Meresse, B., Chen, Z., Ciszewski, C., Tretiakova, M., Bhagat, G., Krausz, T. N., … Jabri, B. (2004). Coordinated induction by IL15 of a TCR-independent NKG2D signaling pathway converts CTL into lymphokine-activated killer cells in celiac disease. *Immunity*, *21*(3), 357–366. https://doi.org/10.1016/j.immuni.2004.06.020

Millington, G. W. M. (2013). Obesity, genetics and the skin. *Clinical and Experimental Dermatology*, *38*(1), 50–56; quiz 56. https://doi.org/10.1111/ced.12024

Mills, R. E., Taylor, K. R., Podshivalova, K., McKay, D. B., & Jameson, J. M. (2008). Defects in skin gamma delta T cell function contribute to delayed wound repair in rapamycin-treated mice. *Journal of Immunology (Baltimore, Md.: 1950)*, *181*(6), 3974–3983.

Mizoguchi, A., Mizoguchi, E., Chiba, C., Spiekermann, G. M., Tonegawa, S., Nagler-Anderson, C., & Bhan, A. K. (1996). Cytokine imbalance and autoantibody production in T cell receptor-alpha mutant mice with inflammatory bowel disease. *The Journal of Experimental Medicine*, *183*(3), 847–856.

Moens, E., & Veldhoen, M. (2012). Epithelial barrier biology: good fences make good neighbours. *Immunology*, *135*(1), 1–8. https://doi.org/10.1111/j.1365-2567.2011.03506.x

Montufar-Solis, D., Garza, T., & Klein, J. R. (2007). T-cell activation in the intestinal mucosa. *Immunological Reviews*, *215*, 189–201. https://doi.org/10.1111/j.1600-065X.2006.00471.x

Müller, S., Bühler-Jungo, M., & Mueller, C. (2000). Intestinal intraepithelial lymphocytes exert potent protective cytotoxic activity during an acute virus infection. *Journal of Immunology (Baltimore, Md.: 1950)*, *164*(4), 1986–1994.

Murano, I., Barbatelli, G., Parisani, V., Latini, C., Muzzonigro, G., Castellucci, M., & Cinti, S. (2008). Dead adipocytes, detected as crown-like structures, are prevalent in visceral fat depots of genetically obese mice. *Journal of Lipid Research*, *49*(7), 1562–1568. https://doi.org/10.1194/jlr.M800019-JLR200

Nelson, J. F., Karelus, K., Felicio, L. S., & Johnson, T. E. (1990). Genetic Influences on the Timing of Puberty in Mice1. *Biology of Reproduction*, *42*(4), 649–655. https://doi.org/10.1095/biolreprod42.4.649

Ogata, M., Ota, Y., Nanno, M., Suzuki, R., & Itoh, T. (2014). Activation of intra-epithelial lymphocytes; their morphology, marker expression and ultimate fate. *Cell and Tissue Research*, *356*(1), 217–230. https://doi.org/10.1007/s00441-013-1786-4

Ogden, C. L., Carroll, M. D., Kit, B. K., & Flegal, K. M. (2014). Prevalence of childhood and adult obesity in the United States, 2011-2012. *JAMA*, *311*(8), 806–814. https://doi.org/10.1001/jama.2014.732

Ogden, C. L., & Flegal, K. M. (2010). Changes in terminology for childhood overweight and obesity. *National Health Statistics Reports*, (25), 1–5.

O'Rourke, R. W., Kay, T., Scholz, M. H., Diggs, B., Jobe, B. A., Lewinsohn, D. M., & Bakke, A. C. (2005). Alterations in T-cell subset frequency in peripheral blood in obesity. *Obesity Surgery*, *15*(10), 1463–1468. https://doi.org/10.1381/096089205774859308

Park, S.-G., Mathur, R., Long, M., Hosh, N., Hao, L., Hayden, M. S., & Ghosh, S. (2010). T regulatory cells maintain intestinal homeostasis by suppressing γδ T cells. *Immunity*, *33*(5), 791–803. https://doi.org/10.1016/j.immuni.2010.10.014

Pennington, D. J., Silva-Santos, B., Shires, J., Theodoridis, E., Pollitt, C., Wise, E. L., … Hayday, A. C. (2003). The inter-relatedness and interdependence of mouse T cell receptor gammadelta+ and alphabeta+ cells. *Nature Immunology*, *4*(10), 991–998. https://doi.org/10.1038/ni979

Perše, M., & Cerar, A. (2012). Dextran sodium sulphate colitis mouse model: traps and tricks. *Journal of Biomedicine & Biotechnology*, *2012*, 718617. https://doi.org/10.1155/2012/718617

Petermann, F., Rothhammer, V., Claussen, M. C., Haas, J. D., Blanco, L. R., Heink, S., … Korn, T. (2010). γδ T cells enhance autoimmunity by restraining regulatory T cell responses via an

interleukin-23-dependent mechanism. *Immunity*, *33*(3), 351–363. https://doi.org/10.1016/j.immuni.2010.08.013

Pickwell, K., Siersma, V., Kars, M., Apelqvist, J., Bakker, K., Edmonds, M., … Schaper, N. (2015). Predictors of lower-extremity amputation in patients with an infected diabetic foot ulcer. *Diabetes Care*, *38*(5), 852–857. https://doi.org/10.2337/dc14-1598

Pi-Sunyer, X. (1998). Executive summary of the clinical guidelines on the identification, evaluation, and treatment of overweight and obesity in adults. *Archives of Internal Medicine*, *158*(17), 1855–1867.

Potten, C. S., Owen, G., Hewitt, D., Chadwick, C. A., Hendry, H., Lord, B. I., & Woolford, L. B. (1995). Stimulation and inhibition of proliferation in the small intestinal crypts of the mouse after in vivo administration of growth factors. *Gut*, *36*(6), 864–873.

Poussier, P., Ning, T., Banerjee, D., & Julius, M. (2002). A unique subset of self-specific intraintestinal T cells maintains gut integrity. *The Journal of Experimental Medicine*, *195*(11), 1491–1497.

Rees, A., Thomas, N., Brophy, S., Knox, G., & Williams, R. (2009). Cross sectional study of childhood obesity and prevalence of risk factors for cardiovascular disease and diabetes in children aged 11-13. *BMC Public Health*, *9*, 86. https://doi.org/10.1186/1471-2458-9-86

Residori, L., García-Lorda, P., Flancbaum, L., Pi-Sunyer, F. X., & Laferrère, B. (2003). Prevalence of co-morbidities in obese patients before bariatric surgery: effect of race. *Obesity Surgery*, *13*(3), 333–340. https://doi.org/10.1381/096089203765887615

Roberts, S. J., Smith, A. L., West, A. B., Wen, L., Findly, R. C., Owen, M. J., & Hayday, A. C. (1996). T-cell alpha beta + and gamma delta + deficient mice display abnormal but distinct phenotypes toward a natural, widespread infection of the intestinal epithelium. *Proceedings of the National Academy of Sciences of the United States of America*, *93*(21), 11774–11779.

Rocha, V. Z., Folco, E. J., Sukhova, G., Shimizu, K., Gotsman, I., Vernon, A. H., & Libby, P. (2008). Interferon-gamma, a Th1 cytokine, regulates fat inflammation: a role for adaptive immunity in obesity. *Circulation Research*, *103*(5), 467–476. https://doi.org/10.1161/CIRCRESAHA.108.177105

Rogol, A. D., Roemmich, J. N., & Clark, P. A. (2002). Growth at puberty. *The Journal of Adolescent Health: Official Publication of the Society for Adolescent Medicine*, *31*(6 Suppl), 192–200.

Rooney, B. L., Mathiason, M. A., & Schauberger, C. W. (2011). Predictors of obesity in childhood, adolescence, and adulthood in a birth cohort. *Maternal and Child Health Journal*, *15*(8), 1166–1175. https://doi.org/10.1007/s10995-010-0689-1

Roscoe B. Jackson Memorial Laboratory, & Green, E. L. (Eds.). (1975). *Biology of the laboratory mouse* (2d ed). New York: Dover Publications.

Saito, H., Kanamori, Y., Takemori, T., Nariuchi, H., Kubota, E., Takahashi-Iwanaga, H., … Ishikawa, H. (1998). Generation of intestinal T cells from progenitors residing in gut cryptopatches. *Science (New York, N.Y.)*, *280*(5361), 275–278.

Schön, M. P., Arya, A., Murphy, E. A., Adams, C. M., Strauch, U. G., Agace, W. W., … Parker, C. M. (1999). Mucosal T lymphocyte numbers are selectively reduced in integrin alpha E (CD103)-deficient mice. *Journal of Immunology (Baltimore, Md.: 1950), 162*(11), 6641–6649.

Schwacha, M. G. (2003). Macrophages and post-burn immune dysfunction. *Burns: Journal of the International Society for Burn Injuries*, *29*(1), 1–14.

Seitz, O., Schürmann, C., Hermes, N., Müller, E., Pfeilschifter, J., Frank, S., & Goren, I. (2010). Wound healing in mice with high-fat diet- or ob gene-induced diabetes-obesity syndromes: a comparative study. *Experimental Diabetes Research*, *2010*, 476969. https://doi.org/10.1155/2010/476969

Shu, L., Beier, E., Sheu, T., Zhang, H., Zuscik, M. J., Puzas, E. J., … Xing, L. (2015). High-fat diet causes bone loss in young mice by promoting osteoclastogenesis through alteration of the bone marrow environment. *Calcified Tissue International*, *96*(4), 313–323. https://doi.org/10.1007/s00223-015-9954-z

Simpson, S. J., Holländer, G. A., Mizoguchi, E., Allen, D., Bhan, A. K., Wang, B., & Terhorst, C. (1997). Expression of pro-inflammatory cytokines by TCR alpha beta+ and TCR gamma delta+ T cells in an experimental model of colitis. *European Journal of Immunology*, *27*(1), 17–25. https://doi.org/10.1002/eji.1830270104

Skrepnek, G. H., Armstrong, D. G., & Mills, J. L. (2014). Open bypass and endovascular procedures among diabetic foot ulcer cases in the United States from 2001 to 2010. *Journal of Vascular Surgery*, *60*(5), 1255–1264. https://doi.org/10.1016/j.jvs.2014.04.071

Solomon, L., Mansor, S., Mallon, P., Donnelly, E., Hoper, M., Loughrey, M., … Gardiner, K. (2010). The dextran sulphate sodium (DSS) model of colitis: an overview. *Comparative Clinical Pathology*, *19*(3), 235–239. https://doi.org/10.1007/s00580-010-0979-4

Speakman, J. R. (2004). Obesity: the integrated roles of environment and genetics. *The Journal of Nutrition*, *134*(8 Suppl), 2090S–2105S.

Steed, H., Walsh, S., & Reynolds, N. (2009). A brief report of the epidemiology of obesity in the inflammatory bowel disease population of Tayside, Scotland. *Obesity Facts*, *2*(6), 370–372. https://doi.org/10.1159/000262276

Tajima, M., Wakita, D., Noguchi, D., Chamoto, K., Yue, Z., Fugo, K., … Nishimura, T. (2008). IL-6-dependent spontaneous proliferation is required for the induction of colitogenic IL-17-producing CD8+ T cells. *The Journal of Experimental Medicine*, *205*(5), 1019–1027. https://doi.org/10.1084/jem.20071133

Taylor, K. R., Costanzo, A. E., & Jameson, J. M. (2011). Dysfunctional γδ T cells contribute to impaired keratinocyte homeostasis in mouse models of obesity. *The Journal of Investigative Dermatology*, *131*(12), 2409–2418. https://doi.org/10.1038/jid.2011.241

Taylor, K. R., Mills, R. E., Costanzo, A. E., & Jameson, J. M. (2010). Gammadelta T cells are reduced and rendered unresponsive by hyperglycemia and chronic TNFalpha in mouse models of obesity and metabolic disease. *PloS One*, *5*(7), e11422. https://doi.org/10.1371/journal.pone.0011422

Theiss, A. L., Fruchtman, S., & Lund, P. K. (2004). Growth factors in inflammatory bowel disease: the actions and interactions of growth hormone and insulin-like growth factor-I. *Inflammatory Bowel Diseases*, *10*(6), 871–880.

The Mouse in Biomedical Research: Diseases. (n.d.).

Toulon, A., Breton, L., Taylor, K. R., Tenenhaus, M., Bhavsar, D., Lanigan, C., … Havran, W. L. (2009). A role for human skin-resident T cells in wound healing. *The Journal of Experimental Medicine*, *206*(4), 743–750. https://doi.org/10.1084/jem.20081787

Uehara, S., Grinberg, A., Farber, J. M., & Love, P. E. (2002). A role for CCR9 in T lymphocyte development and migration. *Journal of Immunology (Baltimore, Md.: 1950)*, *168*(6), 2811–2819.

Uysal, K. T., Wiesbrock, S. M., Marino, M. W., & Hotamisligil, G. S. (1997). Protection from obesity-induced insulin resistance in mice lacking TNF-alpha function. *Nature*, *389*(6651), 610–614. https://doi.org/10.1038/39335

van Wijk, F., & Cheroutre, H. (2010). Mucosal T cells in gut homeostasis and inflammation. *Expert Review of Clinical Immunology*, *6*(4), 559–566. https://doi.org/10.1586/eci.10.34

Visser, M., Bouter, L. M., McQuillan, G. M., Wener, M. H., & Harris, T. B. (1999). Elevated C-reactive protein levels in overweight and obese adults. *JAMA*, *282*(22), 2131–2135.

Visser, M., Bouter, L. M., McQuillan, G. M., Wener, M. H., & Harris, T. B. (2001). Low-grade systemic inflammation in overweight children. *Pediatrics*, *107*(1), E13.

Wabitsch, M. (2000). Overweight and obesity in European children: definition and diagnostic procedures, risk factors and consequences for later health outcome. *European Journal of Pediatrics*, *159 Suppl 1*, S8–13.

Wang, Y., Li, J., Tang, L., Wang, Y., Charnigo, R., de Villiers, W., & Eckhardt, E. (2010). T-lymphocyte responses to intestinally absorbed antigens can contribute to adipose tissue inflammation and glucose intolerance during high fat feeding. *PloS One*, *5*(11), e13951. https://doi.org/10.1371/journal.pone.0013951

Weaning from the breast. (2004). *Paediatrics & Child Health.*, *9*(4), 249–253.

Weisberg, S. P., McCann, D., Desai, M., Rosenbaum, M., Leibel, R. L., & Ferrante, A. W. (2003). Obesity is associated with macrophage accumulation in adipose tissue. *The Journal of Clinical Investigation*, *112*(12), 1796–1808. https://doi.org/10.1172/JCI19246

Whitlock, E. P., Williams, S. B., Gold, R., Smith, P. R., & Shipman, S. A. (2005). Screening and interventions for childhood overweight: a summary of evidence for the US Preventive Services Task Force. *Pediatrics*, *116*(1), e125–144. https://doi.org/10.1542/peds.2005-0242

Wrann, C. D., Laue, T., Hübner, L., Kuhlmann, S., Jacobs, R., Goudeva, L., & Nave, H. (2012). Short-term and long-term leptin exposure differentially affect human natural killer cell immune functions. *American Journal of Physiology. Endocrinology and Metabolism*, *302*(1), E108–116. https://doi.org/10.1152/ajpendo.00057.2011

Xiao, L., Yang, X., Lin, Y., Li, S., Jiang, J., Qian, S., … Li, X. (2016). Large adipocytes function as antigen-presenting cells to activate CD4+ T cells via upregulating MHCII in obesity. *International Journal of Obesity*, *40*(1), 112–120. https://doi.org/10.1038/ijo.2015.145

Xu, H., Barnes, G. T., Yang, Q., Tan, G., Yang, D., Chou, C. J., … Chen, H. (2003). Chronic inflammation in fat plays a crucial role in the development of obesity-related insulin resistance. *The Journal of Clinical Investigation*, *112*(12), 1821–1830. https://doi.org/10.1172/JCI19451

Yang, H., Youm, Y.-H., Vandanmagsar, B., Ravussin, A., Gimble, J. M., Greenway, F., … Dixit, V. D. (2010). Obesity increases the production of proinflammatory mediators from adipose tissue T cells and compromises TCR repertoire diversity: implications for systemic inflammation and insulin resistance. *Journal of Immunology (Baltimore, Md.: 1950)*, *185*(3), 1836–1845. https://doi.org/10.4049/jimmunol.1000021

Yeung, M. M., Melgar, S., Baranov, V., Oberg, A., Danielsson, A., Hammarström, S., & Hammarström, M. L. (2000). Characterisation of mucosal lymphoid aggregates in ulcerative colitis: immune cell phenotype and TcR-gammadelta expression. *Gut*, *47*(2), 215–227.

Yosipovitch, G., DeVore, A., & Dawn, A. (2007). Obesity and the skin: skin physiology and skin manifestations of obesity. *Journal of the American Academy of Dermatology*, *56*(6), 901–916; quiz 917–920. https://doi.org/10.1016/j.jaad.2006.12.004

Zúñiga, L. A., Shen, W.-J., Joyce-Shaikh, B., Pyatnova, E. A., Richards, A. G., Thom, C., … Butcher, E. C. (2010). IL-17 regulates adipogenesis, glucose homeostasis, and obesity. *Journal of Immunology (Baltimore, Md.: 1950)*, *185*(11), 6947–6959. https://doi.org/10.4049/jimmunol.1001269

Zuniga, L. A., Shen, W.-J., Joyce-Shaikh, B., Pyatnova, E. A., Richards, A. G., Thom, C., … Butcher, E. C. (2011). Correction: IL-17 Regulates Adipogenesis, Glucose Homeostasis, and Obesity. *The Journal of Immunology*, *186*(2), 1291–1291. https://doi.org/10.4049/jimmunol.1090126

Zwintscher, N. P., Horton, J. D., & Steele, S. R. (2014). Obesity has minimal impact on clinical outcomes in children with inflammatory bowel disease. *Journal of Pediatric Surgery*, *49*(2), 265–268; discussion 268. https://doi.org/10.1016/j.jpedsurg.2013.11.033